

# The representation of hydrological dynamical systems using Extended Petri Nets (EPN)

Marialaura Bancheri,<sup>1</sup> Francesco Serafin<sup>2</sup> and Riccardo Rigon<sup>2</sup>

<sup>1</sup>Institute for Mediterranean Agricultural and Forestry systems (ISAFOM), National Research Council  
(CNR), Ercolano (NA), Italy

<sup>2</sup>Department of Civil, Environmental and Mechanical Engineering, University of Trento, Trento, Italy

## Key Points:

- We present a graphical system to represent hydrological dynamical systems called Extended Petri Nets (EPN).
- EPN have a one-to-one correspondence with the equations that drive systems.
- EPN topology and connections clarify the causal relationship between compartments and the feedback between them. Two different types of feedback are presented.
- EPN can be used to formalize perceptual models from field work into equations.

---

Corresponding author: Riccardo Rigon, [riccardo.rigon@unitn.it](mailto:riccardo.rigon@unitn.it)

## Abstract

This work presents a new graphical system to represent hydrological dynamical models and their interactions. We propose an extended version of the Petri Nets mathematical modelling language, the Extended Petri Nets (EPN), which allows for an immediate translation from the graphics of the model to its mathematical representation in a clear way. We introduce the principal objects of the EPN representation (*i.e.* places, transitions, arcs, controllers and splitters) and their use in hydrological systems. We show how to cast hydrological models in EPN and how to complete their mathematical description using a dictionary for the symbols and an expression table for the flux equations. Thanks to the compositional property of EPN, we show how it is possible to represent either a single hydrological response unit or a complex catchment where multiple systems of equations are solved simultaneously. Finally, EPN can be used to describe complex earth system models that include feedback between the water, energy and carbon budgets. The representation of hydrological dynamical systems with EPN provides a clear visualization of the relations and feedback between subsystems, which can be studied with techniques introduced in non-linear systems theory and control theory.

## 1 Introduction

In the broad array of hydrological models (Beven, 2011; Wagener et al., 2004) an important category comprises those models that solve systems of Ordinary Differential Equations (ODEs) and their discrete counterparts (for an overview, please refer to Singh and Woolhiser (2002) and Kampf and Burges (2007)). This category includes lumped models, that is to say, models where spatial hydrological variability is integrated over single elements called Hydrological Response Units (HRUs): each HRU represents a certain sub-catchment, while the spatial organization of basins, if required at coarser scales, is obtained by connecting HRUs as nodes of a network. In this case, lumped models are also called “integral distributed models”, (Todini, 1988). In each HRU, a model can treat the internal processes (runoff, evapotranspiration, root zone moisture, and so on) by using one or more ODEs. Therefore, integral distributed models are formed by systems of systems of ODEs.

Not all the aforementioned elements are present in all hydrological models, nor is the same nomenclature used. However, if we take as an example the models collected in the MARRMot 1.0 toolbox (Knoben et al., 2019), we have a substantial group (46) of the most widely used hydrological models, all of which solve ODEs. In literature, (Fenicia et al., 2008; Birkel et al., 2011; Hrachowitz et al., 2013), these Hydrological Dynamical Systems (henceforth HDSys) are used to interpret any of the hydrological processes from hillslope to catchment scale: they are ubiquitous.

The great variety of available models draws attention to the need to find some mathematical criterion for diagnosing their differences (e.g., Clark et al. (2008)). In this paper we suggest that associating an appropriate graphical-mathematical representation to each model can be a part of the diagnostic process.

Graphical representation has been fruitful in the sciences: the epitome is the case of Feynman diagrams in quantum electrodynamics (Kaiser, 2005), but representations of electrical circuits (Lohn & Colombano, 1999), stock-flow diagrams of system dynamics models are also good examples (Takahashi, 2005) and reaction networks (Herajy & Heiner, 2015; Baez & Pollard, 2017) are also interesting examples. The resulting theories, informed by the diagrams, differed significantly from earlier approaches in the way the relevant phenomena were conceptualized and modelled. We believe that devising a graphical representation for hydrological models can also be fruitful, especially if the graphics are more than pictorial representations. As Oster, Perelson, and Katchalsky (1971) suggest, we seek a system where the dynamical equations can be read algorithmically

65 from the graphs and diagrams, which are actually another notation for the equations them-  
 66 selves.

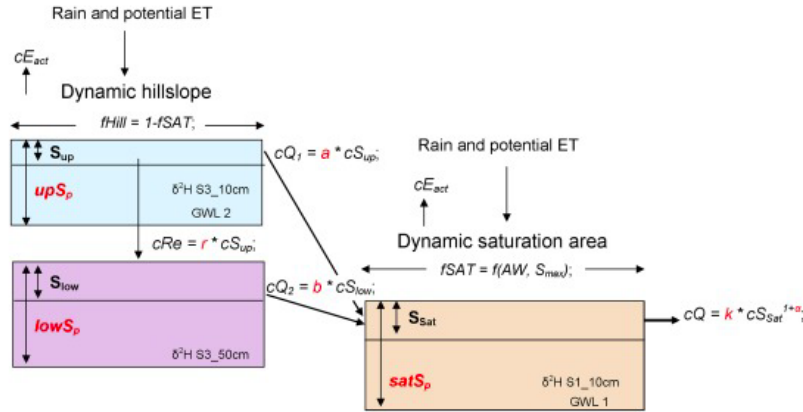
67 In hydrology we have great demands as we deal with various dynamical systems  
 68 besides the water budget, such as the energy budget, the travel time transport of wa-  
 69 ter, and the carbon cycle, to name a few. Therefore, the graphical representation devel-  
 70 oped should be expandable to more than one of the Earth system cycles; it should im-  
 71 ply their mathematics; and it should help visualize their reciprocal feedbacks.

72 In our work, we want to complement the work presented, for instance, in Fenicia  
 73 and Kavetski (2011) and in Clark et al. (2015). Those are papers with a large scope, and  
 74 they treat very broad questions, from how to infer a model's structure using heuristic  
 75 analyses of the functioning catchment (e.g., Butts, Payne, Kristensen, and Madsen (2004))  
 76 to the numerics used in sound, high-performance tools. With respect to the models ad-  
 77 dressed by those papers, the approach of this paper is agnostic: it does not explain how  
 78 to build models but aims to present them in a clear way.

79 In summary, our paper tries to answer the following questions: is there a good way  
 80 to graphically represent budgets (water, energy and other) that gives a clear idea of the  
 81 type of interactions they are subject to before seeing the equations? Where in a graphi-  
 82 cal representation can information about fluxes and parameters be optimally placed?  
 83 Can we obtain a graphic language that corresponds to mathematics in a strict and uni-  
 84 vocal manner? Can the graphical representation help translate the perceptual models  
 85 derived from field work into mathematics and equations? Can we visually represent the  
 86 feedbacks between hydrology and ecosystems?

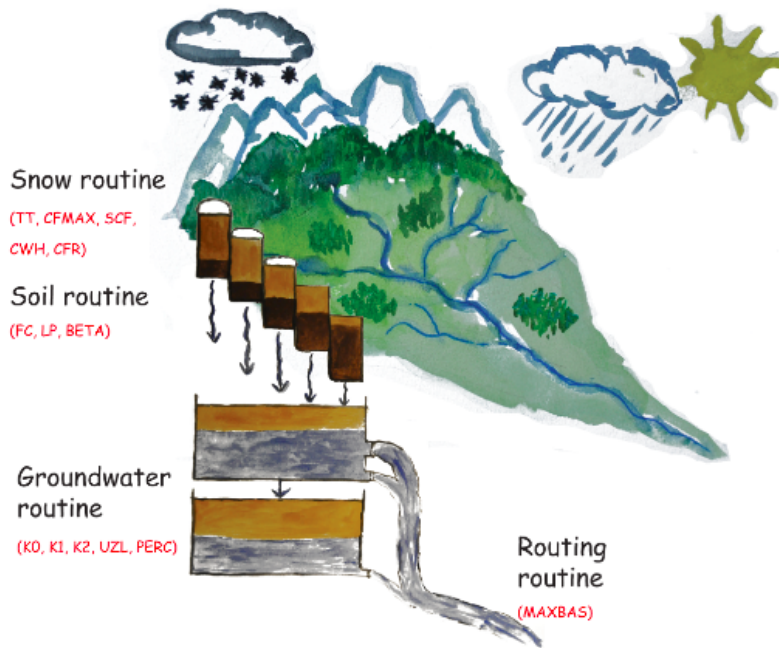
## 87 2 Examples of graphical representation of hydrological models

88 To expound what was said in the Introduction, we reproduce here figures repre-  
 89 senting some well known hydrological models.



90 **Figure 1.** Representation of the model proposed in Birkel et al., (2011). The figure is adapted  
 91 from Soulsby et al. (2016)

92 Figure 1 shows a schematic representation of the model proposed in Birkel et al.  
 93 (2011), which we shall refer to as the BST model (after Birkel, Soulsby, Tetzlaff). In the  
 94 graphic, the relationships between different BST parts are clear; this is not true for the  
 95 fluxes, which have their mathematical expressions annotated in the graphic. Computer



101 **Figure 2.** Hydrologiska Byråns Vattenbalansavdelning (HBV) model as illustrated in Seibert  
 102 and Vis (2012)

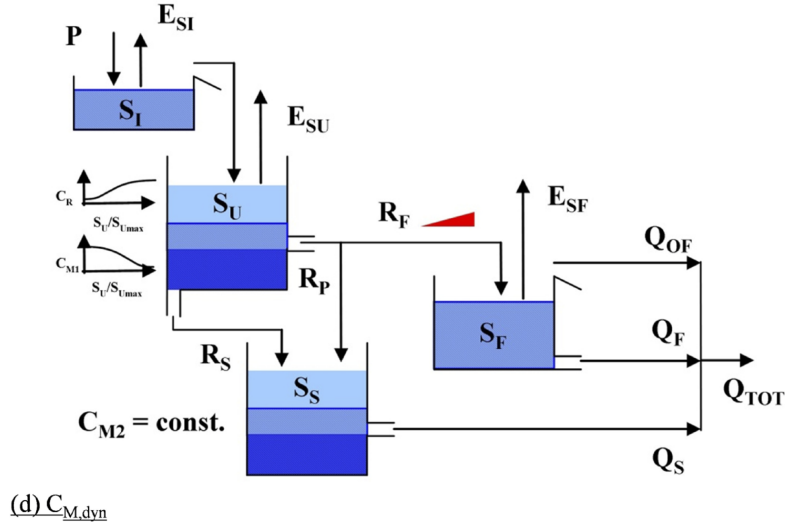
96 scientists would say that the figure has been given too many responsibilities and too much  
 97 information, resulting in a cluttered graphic. To understand and reproduce the BST model,  
 98 decryption work is required in a back and forth process between the image and the text.  
 99 This process is probably unavoidable in all cases, but the reading can be made easier by  
 100 referring to standard places in the manuscript.

103 Figure 2 refers to the Hydrologiska Byråns Vattenbalansavdelning (HBV), adapted  
 104 from Seibert and Vis (2012), a standard reference for HBV. Those Authors opted for a  
 105 pictorial representation that cannot be considered very explicative from a mathemati-  
 106 cal point of view, as it serves to identify the compartments of Earth surface involved.  
 107 While the Figure is very effective in providing an immediate association between the model  
 108 components and their natural counterparts, the interested reader must, however, peruse  
 109 other papers to get all the information needed to understand the workings of the HBV  
 110 model.

113 Figure 3, adapted from Hrachowitz et al. (2013), is one of three model structures  
 114 used in a heuristic procedure (Fenicia et al., 2008) to assess catchment behaviors. The  
 115 figure conveys a lot, but details about flux partition remain unclear. Single reservoirs  
 116 need to act like two or three reservoirs, as represented by the use of different colours. The  
 117 (inattentive) reader could be easily confounded to see only four reservoirs in this model,  
 118 when, instead, the  $S_U$  reservoir should be split in two, and some others are missing too,  
 119 as we shall see later.

120 The model representations in Figures (1) to (3) keep some elements fixed, namely,  
 121 the reservoirs and the arrows. Others elements vary, and some are discarded, in accor-  
 122 dance with the Authors' views. That is to say, it is not possible to gather the main in-  
 123 formation at a glance or, rather, there is no common understanding of what the main  
 124 information to be conveyed is. We cannot easily see the similarities between models, and  
 125 the style changes in representation make any understanding even more difficult.

(b) Loch Ard – Burn 11



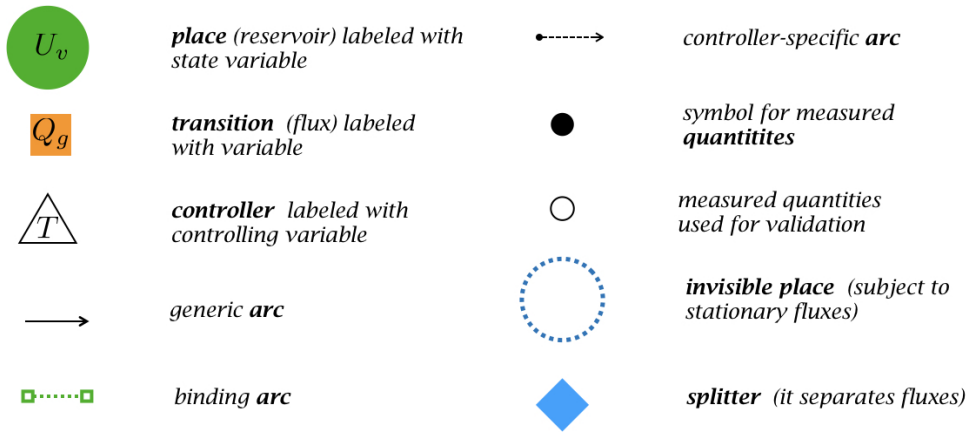
111 **Figure 3.** Representation of one of the models proposed in Hrachowitz et al. (2013), here  
 112 called the Ard-Burn model

126 The goal of this paper is to bring order to HDSys representations by building an  
 127 algebra of graphical objects where any symbol will correspond to a mathematical term  
 128 or group of terms. The main information to be communicated is the number of equa-  
 129 tions that a model uses and the number of input and output fluxes present for each equa-  
 130 tion. At the same time, the number and location of model parameters should be clear,  
 131 but, in our opinion, need not be communicated directly by the graphics.

### 132 3 Principal graphical objects in Extended Petri Networks

133 Among the various possible graphic representation, we find that the Petri Nets (PN)  
 134 are particularly suited to our scope. PN are a mathematical modelling language for the  
 135 description of distributed systems. The concept was originally presented in Carl Adam  
 136 Petri’s dissertation (Petri, 1966) and their early development and applications are found  
 137 in reports that date back to the 1970s. PN became popular in theoretical computer sci-  
 138 ence (Jensen & Kristensen, 2009), biology (Koch, 2010; Koch et al., 2010; Wilkinson, 2011),  
 139 especially to represent parallel or concurrent activities (Murata, 1989), stochastic me-  
 140 chanics (Baez & Biamonte, 2012; Haas, 2006; Marsan et al., 1994) and to describe re-  
 141 action networks (Gilbert & Heiner, 2006; Herajy & Heiner, 2015). In the case of reac-  
 142 tion networks, clearly treated in Herajy and Heiner (2015), there are specific rules for com-  
 143 putation, which are implicit in the PN structure used, that do not lead to correct mass  
 144 and energy budget equations. This matter is referred to in more detail in the supplemen-  
 145 tary material of this paper.

146 Initially, PN were used to model discrete time processes managing discrete, numer-  
 147 able quantities. However, HDSys require a time-dependent form of PN. Such a form is  
 148 already present in literature, (Ramchandani, 1974; Merlin & Farber, 1976; Berthomieu  
 149 & Diaz, 1991; Champagnat et al., 1998; Alla & David, 1998) and is usually called “Time  
 150 Continuous Petri Nets”. These are the generalization of discrete processes that are ap-  
 151 proximated as continuous ones (Silva & Recalde, 2004). However in HDSys, we mostly  
 152 deal with systems of ODEs, where the equations are usually non-linear and the state vari-



168 **Figure 4.** The graphical objects used in EPN. Not all of them need to be present.

153 ables are inherently continuous (mass, energy and momentum of water or other substances).  
 154 Thus we required a different type of PN that we have called Extended Petri Nets (EPN),  
 155 with different rules from, for example, the reaction networks or other typologies of PN.

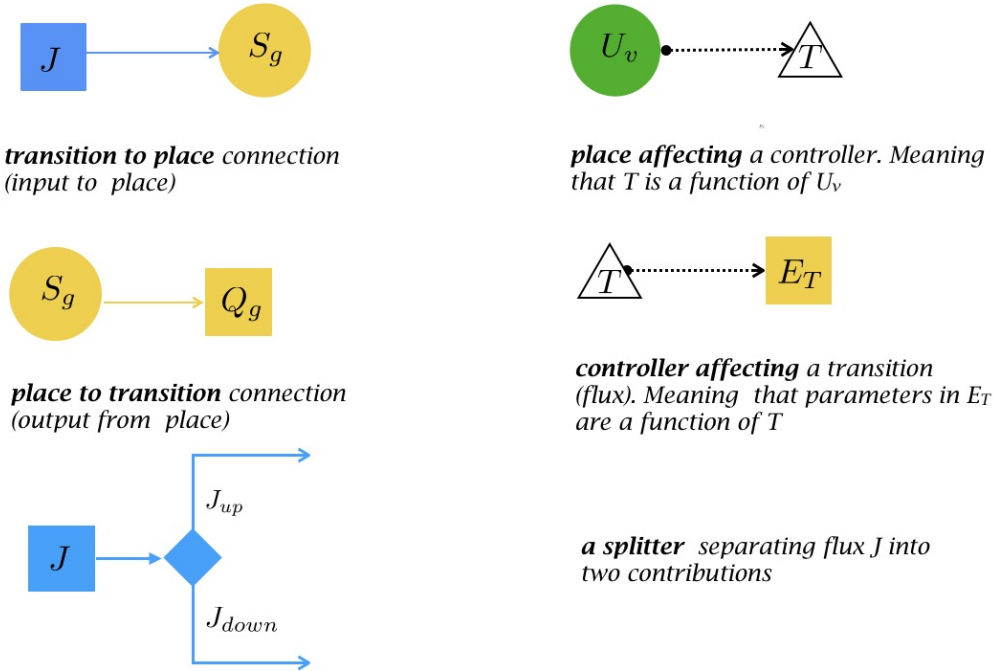
156 When looking at PN, hydrologists must adjust their interpretative habits: reser-  
 157 vvoirs (now called **places**) are represented as circles, and fluxes (now called **transitions**)  
 158 between reservoirs (or places) are represented as squares. To distinguish between differ-  
 159 ent places, the graphical objects can be colored; conventionally, we use the same color  
 160 for places and transitions describing the same compartment, such as, for instance, the  
 161 *soil* or *root zone* as distinct from the *groundwater* zone. The graphical objects have enough  
 162 space for the symbol of the variable they deal with, as shown in Figure 4. A third group  
 163 of objects are the **controllers** (represented by a triangle). They are quantities that af-  
 164 fect fluxes but are not fluxes themselves. Their value can depend on one or more state  
 165 variables, i.e. on places, and they are in charge of regulating fluxes. As an example of  
 166 a controller, consider a mass flux,  $Q$ , proportional to the storage,  $S$ , such that  $Q = kS$ .  
 167 If  $k = k(T)$ , where  $T$  is the temperature, then  $T$  is a controller of the flux.

169 The connection between places and transitions is shown with an **arc**; arcs between  
 170 two places (reservoirs) or between two transitions (fluxes) are not allowed. As shown in  
 171 Figure 4, arcs can be drawn in different ways to convey more detail: if they carry a lin-  
 172 ear flux they are generic and do not include any symbols; if the carry a non-linear flux,  
 173 they are marked by a coloured bullet. Binding arcs are used when two different fluxes  
 174 in two different budgets contain the same variable. That is to say, they join two tran-  
 175 sitions that contain the same variable for graphical reasons, such as, for example, evap-  
 176 otranspiration in the water and energy budgets, as shown in section 7. Oriented dashed  
 177 arcs show connections from places to controllers and from controllers to transitions. Con-  
 178 nections between places and transitions that pass trough controllers only affect the ex-  
 179 pression of fluxes but do not alter the number of equations. Any oriented arc also rep-  
 180 represents a causal relation between the originating entity and the receiving one: upstream  
 181 quantities can be thought to cause downstream ones. Therefore the controllers show the  
 182 causal relationship between state variables and fluxes, which would otherwise be hidden  
 183 graphically. For this reason we call the wiring from places to controllers to transitions  
 184 hidden wiring or **h-wiring**, while the wiring that connects directly between places and  
 185 transitions is called flux wiring or **f-wiring**.

186 In Figure 4 we also introduce a small, solid, black circle, which is used to mark a  
 187 measured quantity, i.e. a quantity that is given as known input and drives the simula-  
 188 tion. The most common example of known input is precipitation, which is usually ob-

189 tained from ground measurements or other sources. The small, empty circle represents  
 190 a quantity that is also given but is used to assess the goodness of the model. In hydrology,  
 191 the typical case is the discharge, which is an output of the models and whose measured  
 192 values are used for validation. The big circle with the dotted border represents instead  
 193 a hidden place whose budget is stationary, as it returns all the mass it takes in.  
 194 A typical example in hydrological models is that of uphill surface waters and ground-  
 195 waters summing to give the total surface discharge.

196 All the allowable connections between EPN objects are represented in Figure 5; no  
 197 other type of connection is possible. A transition can be connected to more than one place,  
 198 implying the existence of a partition coefficient, represented by a **splitter** (the diamond  
 199 symbol in Figure 4). For instance, the total amount of precipitation can be divided into  
 200 snowfall and rainfall, or between two reservoirs representing surface waters and the root  
 201 zone. In those cases the splitter represents the need for some rule to separate the fluxes.  
 202 Figure 5 shows a splitter in action, where precipitation  $J$  is divided into 2 components,  
 203  $J_{up}$  and  $J_{down}$ . In the case presented in section 4.1, the separation is simply obtained  
 204 with a partition coefficient, for which  $\alpha$  part of the precipitation goes into a *surface reser-*  
 205 *voir* and  $(1-\alpha)$  part goes to a *soil reservoir*. Usually, however, each internal transition  
 206 is connected to only one place. Similarly, a place can be connected to more than one tran-  
 207 sition, also implying a partitioning rule or coefficient. Two places cannot be connected  
 208 to a unique transition, and this marks a substantial difference with reaction networks  
 209 (Gilbert & Heiner, 2006), as shown in detail in the supplementary material of this pa-  
 210 per.



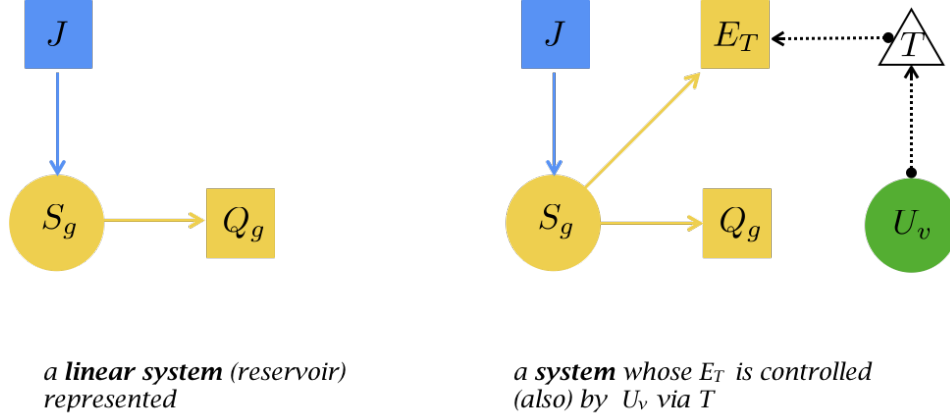
211 **Figure 5.** Allowed connectivity between places, transitions and controllers, and a splitter in  
 212 action. No other type of connection is possible.

To obtain the required budget equations, each place depicted in Figures 4 and 5 must correspond to the time variation of the quantity indicated in it. For instance, the green place marked  $U_v$  represents the following part of a conservation equation:

$$\frac{dU_v}{dt} \tag{1}$$



214 with the quantity  $U_v$  being, for instance, the internal energy of a compartment of the  
 215 HDSys. The differential operator can be changed for other operators, depending on the  
 216 type of equation we are writing, and, therefore a table defining which differential oper-  
 217 ator we are using is needed. From these rules we can represent a simple linear reservoir,  
 as shown in Figure 6 on the left.



213 **Figure 6.** A simple linear reservoir (on the left) and a more complex example (on the right).

218

In Figure 6 the flux  $J$  enters the place  $S_G$ , while the flux  $Q_G$  exits the same place. Therefore the budget is read as:

$$\frac{dS_g}{dt} = J(t) - Q_g(t) \tag{2}$$

Introducing another outgoing flux into the system, as shown on the right in Figure 6, the equation is modified to:

$$\frac{dS_g}{dt} = J(t) - Q_g(t) - E_T(t) \tag{3}$$

219 The action of the controller  $T$  on  $E_T$  remains hidden until we specify the mathemati-  
 220 cal form of the fluxes (transitions). This will be shown with the reference cases in the  
 221 next section and mathematically formalized in section 8.

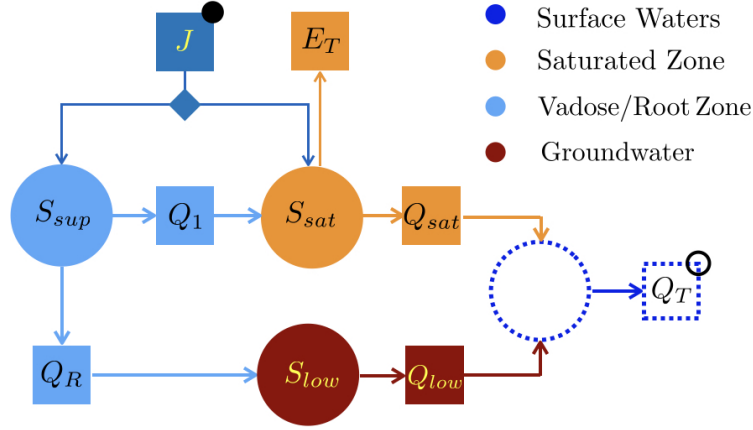
## 222 4 Casting the BST, HBV and Ard-Burn models into the EPN repre- 223 sentation

224 Applying the rules introduced in section 3, we can now represent the three mod-  
 225 els of section 2 using EPN. We will present the details for the BST model, while we will  
 226 be more concise for the others.

### 227 4.1 The BST model

234 As a result of the rules introduced in Section 3, the BST model, shown in Figure  
 235 1, can be represented using EPN as shown in Figure 7. It shows three coupled ODEs,  
 236 represented by three places, colored light blue, orange and dark red (colors chosen to be  
 237 colorblind friendly, as better explained in the supplementary material). The small black  
 238 bullets indicate quantities that should be measured and, therefore, assigned externally.  
 239 A fourth, unnamed place has been added to highlight that measured data refers to the  
 240 total flux,  $Q_T = Q_{sat} + Q_{low}$ , and not the two fluxes separately. This place is, in a sense,





228 **Figure 7.** Representation of the BST model (Birkel et al., 2011) using EPN. Compared with  
 229 the original representation of Figure 1, this Figure contains less information, however, it is suf-  
 230 ficient to write down the mass conservation equations for the system. The invisible reservoir  
 231 is unnamed, since it is just the sum of  $Q_{low}$  and  $Q_{sat}$  and does not store water. As the legend  
 232 shows, each color refers to a different conceptual-physical compartment through which the water  
 233 flows. The outcomes from the splitter are named according to Table 1.

241 invisible because it does not introduce any ODE and its storage variation is always null;  
 242 it has been left nameless and shown with dashed borders to reinforce this concept.

From the graph in Figure 7, the ruling equations are easily written as:

$$\frac{dS_{sup}(t)}{dt} = \underbrace{\alpha J(t)}_{J_l} - Q_1(t) - Q_R(t) \quad (4)$$

243 for the “sup” storage;

$$\frac{dS_{sat}(t)}{dt} = \underbrace{(1 - \alpha)J(t)}_{J_r} + Q_1(t) - Q_{sat}(t) - E_T(t) \quad (5)$$

244 for the “sat” storage; and

$$\frac{dS_{low}(t)}{dt} = Q_R(t) - Q_{low}(t) \quad (6)$$

245 for the “low” storage.

Finally

$$0 = Q_T(t) - Q_{low}(t) - Q_{sat}(t) \quad (7)$$

246 In the BST model, there is one given (measured) input, precipitation  $J$ , which splits  
 247 into  $J_l$  and  $J_r$ , and one given output,  $Q_T$ , each of which is marked with a small circle  
 248 in Figure 7. One of the equations (the “orange” one, Eq. 5) contains a non-linear term,  
 249 while the others are linear. Figure 7 is not sufficient to implement the model because  
 250 its role (responsibility) is to identify the number of equations and to allow the reader to  
 251 write the water budgets with unspecified fluxes. For complete information, two other el-  
 252 ements are needed:

- 253 • a **dictionary** giving the names of the symbols in the graphic (conveying their mean-  
 254 ing), given in Table 1; and

- 255 • an **expression table** giving mathematical completeness to the fluxes, presented  
 256 in Table 2 . When there is a splitter, the corresponding flux is duplicated as nec-  
 257 essary.

258 Expressions for places are not reported here since, by default, they associate any vari-  
 259 able  $S_*$  to its time derivative  $dS_*/dt$ . However, in the most complex cases it is required  
 260 to report them. Because the specification of fluxes usually introduces new variables, an  
 261 extension to the dictionary may be necessary after writing the expression table. The sub-  
 262 stitution of the expressions in Table 2 into equations 4 to 7 gives the set of equations nec-  
 263 essary to fully reproduce the model.

264 **Table 1.** Full dictionary associated to the EPN representation of the BST model (Birkel et  
 265 al., 2011).  $P$  stands for “parameter”,  $F$  for “flux”,  $SV$  for “state variable”,  $V$  for “variable”. [T]  
 266 stands for time units, [L] for length units, [E] for energy units. It contains the symbols present in  
 267 Figure 7 and also those implied by Table 2

Symbol	Name	Type	Unit
$a$	linear reservoir coefficient	P	$[T^{-1}]$
$b$	non-linear reservoir coefficient	P	$[T^{-1}]$
$c$	non-linear reservoir exponent	P	$[-]$
$d$	linear reservoir coefficient	P	$[T^{-1}]$
$e$	linear reservoir coefficient	P	$[T^{-1}]$
$f$	dimensional ET coefficient	P	$[E^{-1}L^5]$
$E_T(t)$	evapotranspiration	F	$[L^3T^{-1}]$
$J^\bullet(t)$	precipitation rate	F	$[L^3T^{-1}]$
$J_l(t)$	precipitation rate going into $S_{sup}$	F	$[L^3T^{-1}]$
$J_r(t)$	precipitation rate going into $S_{sat}$	F	$[L^3T^{-1}]$
$Q_1(t)$	discharge from the upper reservoir	F	$[L^3T^{-1}]$
$Q_{low}(t)$	discharge from the lower reservoir	F	$[L^3T^{-1}]$
$Q_{sat}(t)$	discharge from the saturated reservoir	F	$[L^3T^{-1}]$
$Q_R(t)$	recharge term of the lower reservoir	F	$[L^3T^{-1}]$
$Q_T^o(T)$	total discharge at the outlet	F	$[L^3T^{-1}]$
$R_n(t)$	net radiation	F	$[EL^{-2}T^{-1}]$
$S_{low}(t)$	storage in the lower reservoir	SV	$[L^3]$
$S_{max}(t)$	maximum storage in the saturated reservoir	SV	$[L^3]$
$S_{sat}(t)$	storage in the saturated reservoir	SV	$[L^3]$
$S_{sup}(t)$	storage in the upper reservoir	SV	$[L^3]$
$t$	time	V	[T]
$\alpha$	partitioning coefficient	P	$[-]$

270 Table 2 clarifies the parameters of the model:

- 271 •  $J(t)$  is an external measured quantity (thus it is marked with a bullet,  $\bullet$ );  
 272 • Only five parameters ( $a, b, c, d, e$ ) are necessary since  $E_T$  is also assumed measured  
 273 (as per original paper).

#### 274 4.2 The HBV model

275 As another example, let us consider the EPN representation of the HBV model,  
 276 shown in Figure 8. The HBV model was first shown in Figure 2 in Section 2. Tables A.1  
 277 and A.2 in Appendix A contain the associated dictionary and expression table.

268 **Table 2.** Expression table associated to the EPN representation of the BST model(Birkel et  
 269 al., 2011). Quantities marked with bullets represent measured quantities.

Flux	Name	Expression
$ET(t)$	evapotranspiration	$ET(t)$
$J^\bullet(t)$	precipitation rate	$\bullet$
$J_l(t)$	precipitation rate going into $S_{sup}$	$\alpha J^\bullet(t)$
$J_r(t)$	precipitation rate going into $S_{sat}$	$(1 - \alpha)J^\bullet(t)$
$Q_{up}(t)$	discharge from the upper reservoir	$aS_{sup}(t)$
$Q_{low}(t)$	discharge from the lower reservoir	$dS_{low}(t)$
$Q_{sat}(t)$	discharge from the saturated reservoir	$bS_{sat}(t)^c$
$Q_R(t)$	recharge term of the lower reservoir	$eS_{up}(t)$
$Q_T^o(t)$	total discharge at the outlet	$Q_{sat} + Q_{low}$

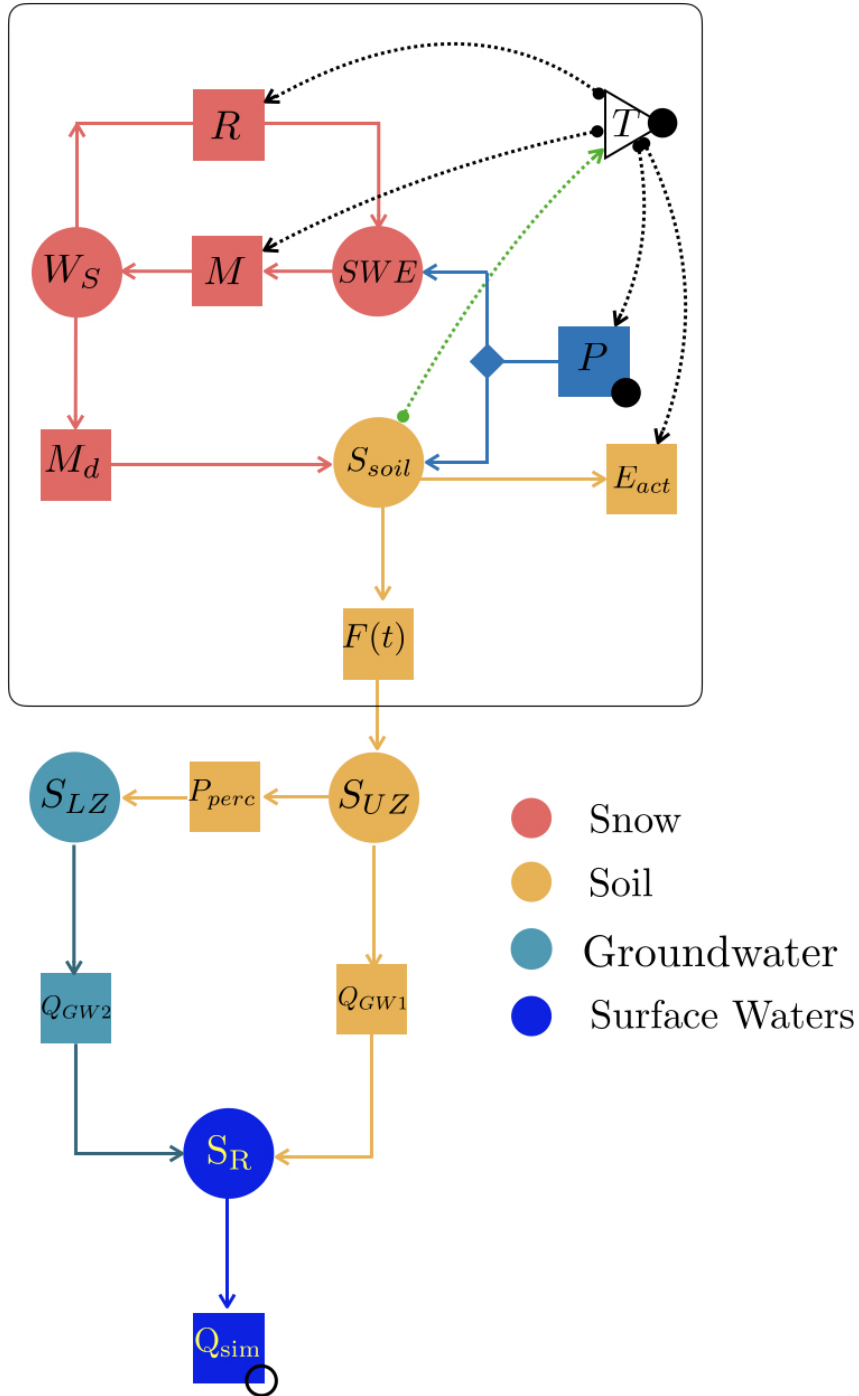
278 The HBV model identifies four major compartments, snow (red), soil (yellow), ground-  
 279 water (cyan) and surface waters (bright blue), as well as precipitation. It contains six  
 280 ODEs and, in contrast with the BST, it also contains a loop between  $SWE$  (snow wa-  
 281 ter equivalent) and  $W_s$  (liquid water in snow). This loop implies that the output of liq-  
 282 uid water from snow can refreeze and increase the amount the snow water equivalent from  
 283 which melted water derives and, by definition, adds a feedback to the system. This causes  
 284 some complications for the resolution of the model at the numerical level. In fact, parts  
 285 of graphs within loops have to be solved simultaneously with an iterative method (Carrera  
 286 et al., 2005; Patten et al., 1990), which usually requires an overhead in computation pro-  
 287 portional to the number of elements in the loop.

288 A new feature appearing in the HBV model representation is the introduction of  
 289 a controller. The triangle marked with  $T$  shows explicitly that temperature controls vari-  
 290 ous fluxes, as made clear in Expression Table A.2: Actual Evapotranspiration,  $E_{act}$ , pre-  
 291 cipitation,  $P$ , melting rate of snow,  $M$ , and refreezing rate of the liquid water in the snow-  
 292 pack,  $R$ , are all controlled by temperature. For illustrative purposes, a fictitious depen-  
 293 dence of  $T$  on  $S_{soil}$  has been added, with the scope of introducing controller dependent  
 294 loops, which will be detailed in section 8.

### 300 4.3 The Loch Ard-Burn model

301 Finally, Figure 9 represents the Loch Ard-Burn model in Hrachowitz et al. (2013),  
 302 i.e. the model first shown in Figure 3 of Secton 2. The model has four major compart-  
 303 ments: interception by vegetation (in green), an unsaturated reservoir (dark orange), a  
 304 fast reservoir (light blue), a slow reservoir (dark blue). In this case we, the Authors, have  
 305 preferred to identify the compartments with process names rather than locations and,  
 306 in a sense, this is also the choice in the perceptual model of the catchment. Compared  
 307 to the original representation, we have added three new reservoirs: the invisible  $S_O$ , and  
 308  $X_F$  and  $X_S$ .  $S_O$  makes sense of the fluxes  $R_p$  and  $R_s$  that otherwise would both go from  
 309  $S_{SU}$  into  $S_S$  without identifying them properly. In fact, the use of different kinds of blue  
 310 in the original representation in Figure 3 implies the existence of this reservoir. Hrachowitz  
 311 et al. (2013) introduced it to adjust the simulated water age to that measured with trac-  
 312 ers.  $S_O$  does not accumulate water, implying that  $R_S = R_O$ , with a null net water bud-  
 313 get exchange between  $S_O$  and  $S_{SU}$  reservoirs, but it mixes the younger water of the up-  
 314 per reservoirs with older waters to get the right water age at the budget. This trick was  
 315 used before in (Fenicia et al., 2010) and we shall not discuss it fully here.

In Hrachowitz et al. (2013) the discharges  $R_F$  and  $R_P$  from the unsaturated reser-  
 voirs seem to go to reservoirs  $S_F$  and  $S_S$ . However, these actually receive inputs  $R_F^*$  and



295 **Figure 8.** Representation of the HBV model in (Seibert & Vis, 2012). It contains six reser-  
 296 voirs - ODEs - and an external controller of various fluxes, the temperature  $T$ . The black bullets  
 297 indicate that  $P$ ,  $T$  and  $Q_{sim}$  are measured quantities:  $T$  and  $P$  are used for running the model,  
 298 while  $Q_{sim}$  is usually used for calibration/validation. For the meaning of the symbols, please  
 299 refer to the dictionary in Table A.1.

$R_P^*$ , which are the result of a convolution of  $R_F$  and  $R_P$  with some unit hydrographs. All of this implies the existence of additional reservoirs (places) to accommodate a wa-

ter budget. For example, the discharges  $R_F$  and  $R_F^*$  are associated to the budget:

$$\frac{dX_F}{dt} = R_F - R_F^* \quad (8)$$

where the expression of the discharges is given in Table B.1 in Appendix B. In particular:

$$R_F^* = \int_0^t h_F(t - t_{in}) R_F(t_{in}) dt_{in} \quad (9)$$

316 where  $h_f$  is a instantaneous unit hydrograph whose expression is:

$$h_F(t) = \begin{cases} 1/2t/T_F^2 & 0 < t < T_F \\ 0 & otherwise \end{cases} \quad (10)$$

317 where  $t$  is time and  $T_F$  is a suitable parameter.

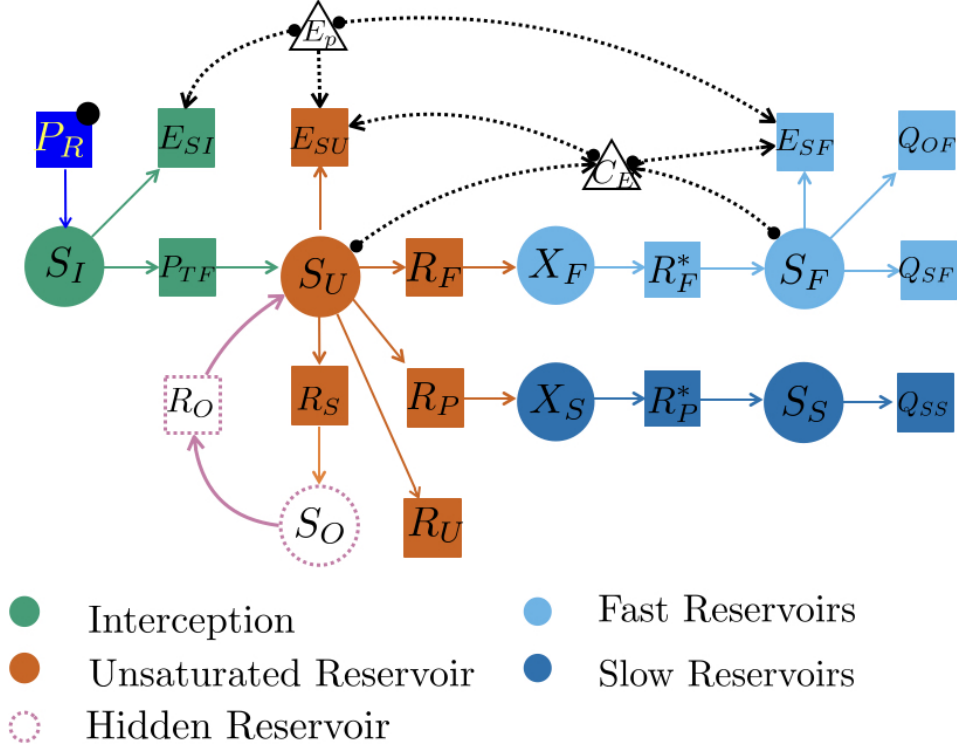
318 One might question whether this is the simplest modelling structure accounting for  
 319 tracer measurements and whether the place  $S_{SO}$  is necessary to have proper water ages  
 320 at the outlet. We merely observe that the representation in Figure 9 explicits this more  
 321 clearly than Figure 3. Besides, Figure 3 ignores the existence of the discharge  $R_U$ , which  
 322 is necessary to preserve the mass budget of the unsaturated reservoir  $S_{SU}$ . It is worth  
 323 noting how the inclusion of controllers in the EPN representation shows clearly the im-  
 324 portance of potential evapotranspiration  $E_p$  and the  $C_E$  parameter (a function of stor-  
 325 ages  $S_{SU}$  and  $S_F$ ) on evapotranspiration; otherwise, this would only be apparent by a  
 326 careful inspection of the flux expressions. The Dictionary and Tables for the Ard-Burn  
 327 model are presented in Appendix B.

## 332 5 Use of Petri Nets for interpreting field work

338 EPN can be used during the “perceptual phase” of research that moves from ex-  
 339 perimental evidence to the construction of an appropriate numerical model of a catch-  
 340 ment. This can be done either according to the strategies defined in Fenicia and Kavet-  
 341 ski (2011) and Clark et al. (2015), or with a more qualitative procedure, like the one we  
 342 follow here, which represents just one practical application of EPN’s functionalities. As  
 343 an example, we can take the description of the Maimai catchment (Gabrielli et al., 2018),  
 344 which is probably among the most widely studied small catchments in the world. The  
 345 dynamics of the catchment is described as: “Catchment storage is formed by two sharply  
 346 contrasting and distinct hydrological units: shallow, young soil storage, and deep, much  
 347 older bedrock groundwater”. Therefore, there are at least two storage reservoirs. The  
 348 description then continues: “This storage pairing produces a bimodal, seasonal stream-  
 349 water”. This means that streams are a third reservoir that collect water from the other  
 350 two, the soil and groundwater reservoirs. It then states that during the summer months  
 351 there is evapotranspiration,  $E_T$ , and that it is an important term of the water budget.  
 352 In a conceptual model  $E_T$  can only come from the soil reservoir. The groundwater reser-  
 353 voir contributes to surface waters and downstream storage. A proper description of the  
 354 catchment should also include the effects of interception and evaporation from the canopy;  
 355 however, for simplicity, these are not taken into account here.

356 From this description, then, it seems that the perceptual model can be instanti-  
 357 ated with two EPN places, which correspond to a set of two main ordinary differential  
 358 equations, as shown in Figure 10. Because of its similarity with the system proposed by  
 359 Kirchner (2016), we have used the names introduced in that paper, with the exception  
 360 of evapotranspiration,  $E_{T_s}$ , and percolation,  $R_l$ , which we have added.

363 Another reservoir can be added to account for surface water storage where ground-  
 364 water and soil water mix. This reservoir is where the fluxes  $\check{L}$  and  $Q_l$  are summed and,  
 365 as such, it is an invisible place. The dictionary for this system is presented in Table 3.

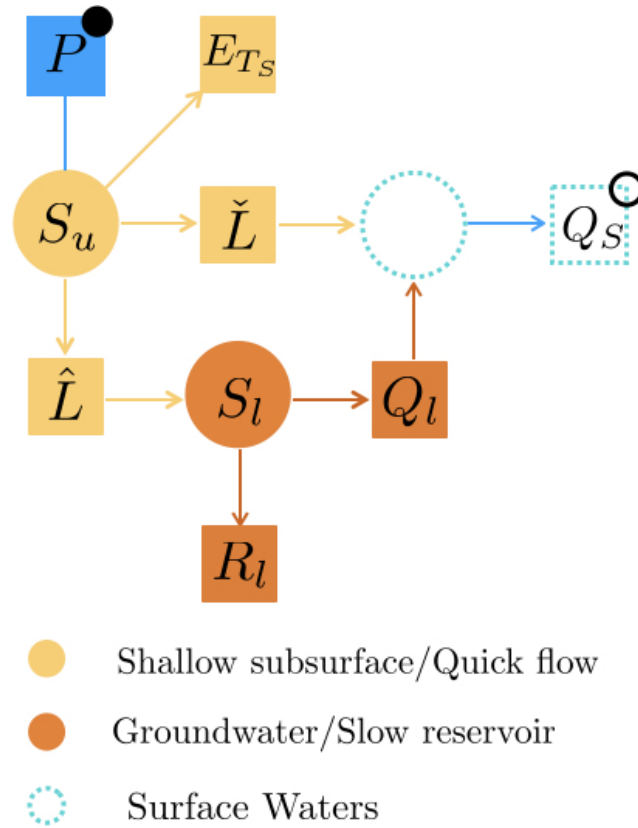


328 **Figure 9.** EPN representation of the Ard-Burn model, corrected for proper water age tracking.  
 329 It has seven main water budget equations, derived from an accurate reading of Hrachowitz  
 330 et al. (2013). The red dotted reservoir,  $S_O$ , is added to account properly for tracer history. The  
 331 bluish reservoirs account for lag times from  $S_{SU} \rightarrow S_F$  and  $S_{SU} \rightarrow S_S$ .

361 **Table 3.** Dictionary for the Maimai catchment model.  $F$  indicates “flux”;  $SV$  “state variable”;  
 362  $V$  “variable”. Quantities marked with bullets represent measured quantities.

Symbol	Name	Type	Units
$E_{T_s}(t)$	Evapotranspiration from the soil reservoir	F	$[L T^{-1}]$
$\dot{L}(t)$	Discharge from soil	F	$[L T^{-1}]$
$\hat{L}(t)$	Recharge to groundwater	F	$[L T^{-1}]$
$P^\bullet(t)$	Precipitation	F	$[L T^{-1}]$
$Q_l(t)$	Discharge from groundwater	F	$[L T^{-1}]$
$Q_S^g(t)$	Total discharge	F	$[L T^{-1}]$
$R_l(t)$	Percolation to a deeper aquifer	F	$[L T^{-1}]$
$S_l(t)$	Storage in the groundwater reservoir	SV	$[L]$
$S_u(t)$	Storage in the soil reservoir	SV	$[L]$
$t$	time	V	$[T]$

366 To understand how to write the tentative equations for such a system, we need to fur-  
 367 ther clarify the semantics of the graph, i.e. we need to make the mathematical structure  
 368 of the fluxes explicit. For this one can find inspiration in Kirchner (2016) but we do not  
 369 pursue it further here.



333 **Figure 10.** EPN representation of the Maimai catchment according to our reconstruction. It  
 334 has two main reservoirs, a soil reservoir,  $S_u$ , and a groundwater reservoir,  $S_l$ . There is also a sur-  
 335 face water reservoir,  $S_{sup}$ , where soil waters and groundwater mix without any delay (so it is an  
 336 invisible place). In Gabrielli et al. (2018) soil water fluxes and groundwater fluxes were measured  
 337 separately and, therefore, we mark them with a black bullet.

## 370 6 Modeling Hydrology as an Earth System Science

371 The HDSys are open dynamical systems that exchange water and energy with their  
 372 surroundings. They are non-linear and usually non-autonomous, they have non-trivial  
 373 time-dependent properties and, being open systems, their future inputs are unknown.  
 374 Therefore, they differ from the dynamical systems treated in other disciplines where, for  
 375 instance, forcings can be written as periodic functions (a typical example in textbooks  
 376 is Strogatz (1994)).

377 One of the contemporary directions of hydrological research is to investigate HDSys  
 378 as part of the larger Earth system science, which includes, among others, the energy and  
 379 carbon cycles. Thus, the hydrological cycle becomes part of a broader living environment  
 380 that feeds back on itself (H. H. G. Savenije & Hrachowitz, 2017; Zehe et al., 2014). Ecosys-  
 381 tems are not passive spectators of hydrological events but co-evolve with hydrology (H. G. Savenije  
 382 & Hrachowitz, 2017). According to this concept, ecosystems control the hydrological cy-  
 383 cle (and vice versa, of course). To be able to represent such complexities, we have to en-  
 384 sure that EPN can represent the energy budget and vegetation growth just as well as  
 385 it represents the water budget. For these aspects, clearly, the usual representation of a  
 386 model as a complex of reservoirs falls short.



387

### 6.1 The energy budget of a simple system

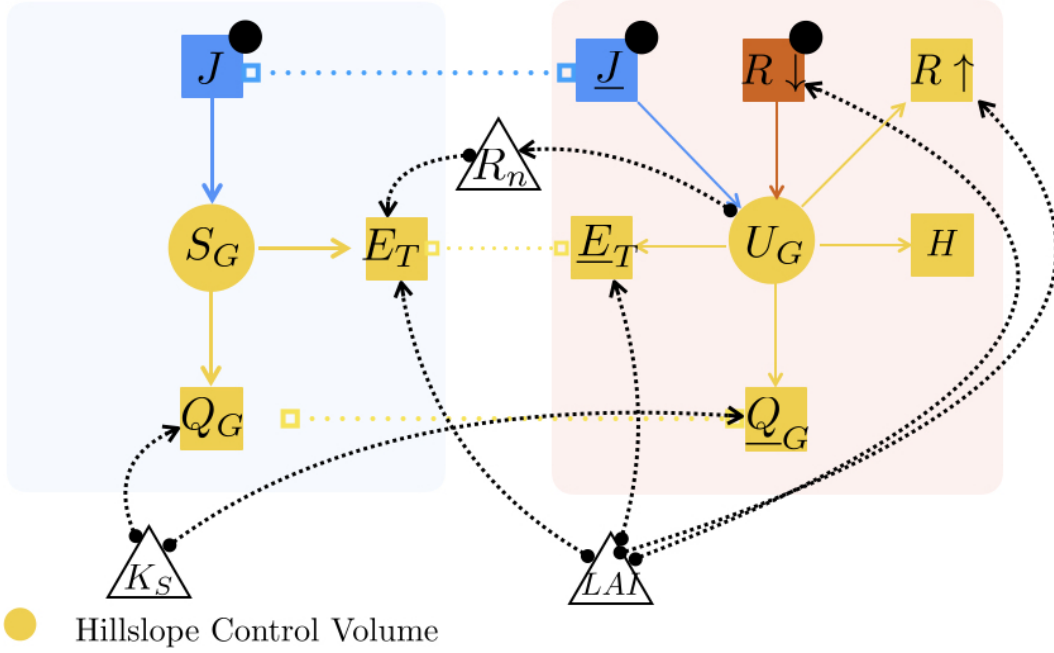


**Figure 11.** Coupled energy and water budgets. The graphic notation is enriched with the addition of a new type of arc (dotted segments ending in empty squares). These arcs connect the same variables present in both budgets. In this case, the  $J$ 's are input, while the  $E_T$ 's and  $Q_G$ 's are unknown variables that must be solved simultaneously in both budgets. Because  $E_T$  depends on radiation, a controller exiting from the  $U_G$  place is added to reveal this further influence of the energy budget on the water budget. Other controllers of the system can be the leaf area index, LAI, which controls radiation and evapotranspiration, and hydraulic conductivity,  $K_S$ , which can be thought to influence flow  $Q_G$ .

Rarely has the energy budget been present in hydrological models so far. Current studies, covering the whole set of hydrological fluxes (e.g. Abera, Formetta, Brocca, and Rigon (2017); Kuppel, Tetzlaff, Maneta, and Soulsby (2018)), require that both the water and energy budgets be solved. To describe this coupling we use the simple example shown in Figure 11(left), referring to a hillslope water budget, with the the associated energy budget also shown in Figure 11(right). To distinguish between the budgets, we used a further graphical stratagem in the figure and colored the background light pastel blue for the water budget and light pastel red for the energy budget).

The dictionary associated to the graph in Figure 11 (left) is in Table 4 and the budget can be deduced to be:

$$\frac{dS_g(t)}{dt} = J(t) - E_T - Q_g \quad (11)$$

The Expression Table is not needed at present and has been omitted.

In Figure 11(right), one can observe that the internal energy of the control volume contains one energy flux for each water flux present in the water budget. In fact, each mass flux has an associated internal energy, conveniently represented as enthalpy per unit mass, which flows in or out when mass is acquired or lost by the control volume. Thus, for instance, given the rainfall  $J$ , the corresponding enthalpy flux is  $\underline{J} = \rho_w h_w J$ , where  $\rho_w$  is the water density in the volume, and  $h_w$  is the water enthalpy per unit mass. In

405 **Table 4.** Dictionary **d** relative to Figure 11. The underscoring (·) represents the internal en-  
 406 ergy acquired or lost through mass exchanges.

Symbol	Name	Type	Unit
[E]	energy per unit area	-	[E]
$E_T(t)$	evapotranspiration	F	$[LT^{-1}]$
$\underline{E}_T(t)$	evapotranspiration energy content	F	$[EL^{-2}]$
$H$	sensible heat	F	$[ET^{-1}]$
$J^\bullet(t)$	precipitation rate	F	$[LT^{-1}]$
$\underline{J}^\bullet(t)$	precipitation energy content	F	$[ET^{-1}]$
$\underline{Q}_g(t)$	discharge	F	$[L^3T^{-1}]$
$\underline{Q}_g(t)$	discharge internal energy	F	$[ET^{-1}]$
$\underline{R}^\bullet \downarrow$	incoming radiation	F	$[ET^{-1}]$
$R \uparrow$	outgoing radiation	F	$[ET^{-1}]$
$S_g(t)$	water storage	SV	$[L^3]$
$t$	time	V	[T]
$U_g$	internal energy	SV	[E]

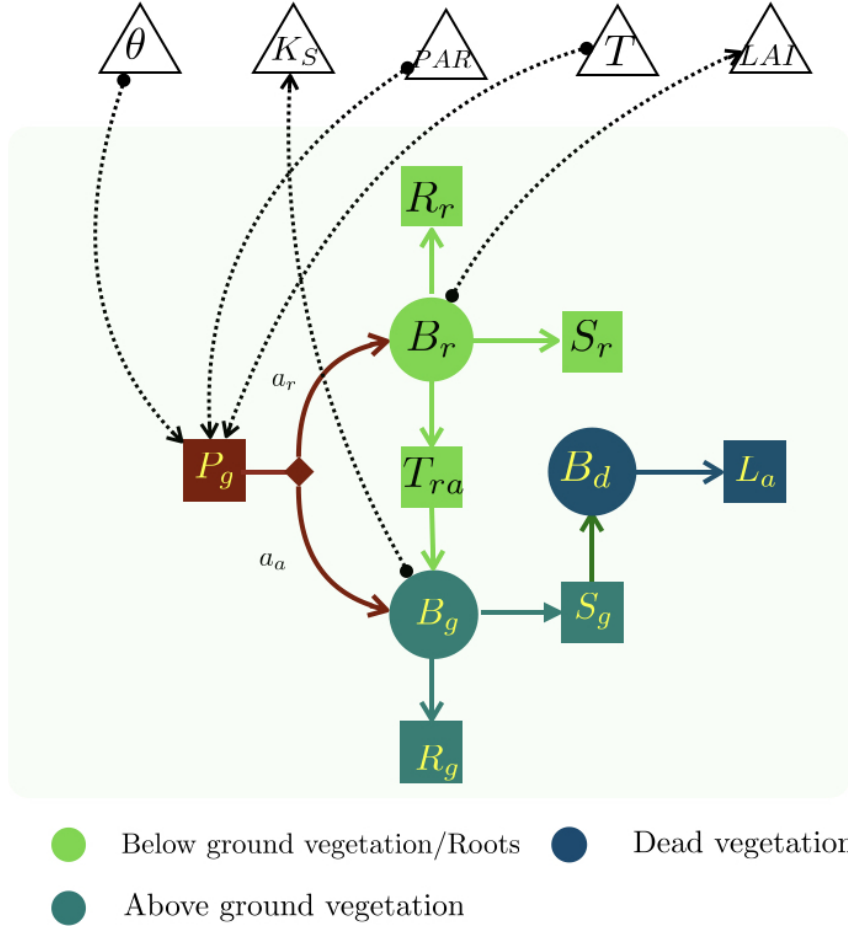
short, many variables are common to both budgets, i.e. they are shared by the budgets and must satisfy both of them. These variables are joined by a new type of arc, a dotted segment capped with empty squares. In addition to these variables, in the energy budget we have to account for the radiation budget, written here as the budget of incoming  $R \downarrow$  and outgoing,  $R \uparrow$  radiation associated to the place  $U_G$ . Latent heat is accounted for as evapotranspiration multiplied by the latent heat (enthalpy) of vaporization. Finally, the energy flux due to thermal energy exchange by convection (sensible heat), flux  $H$ , is taken into account. The resulting energy budget equation is:

$$\frac{dU_G}{dt} = \underline{J} + R \downarrow - R \uparrow - \underline{E}_T - H - \underline{Q}_G \quad (12)$$

407 **Table 5.** Expression table **E** relative to the energy exchange model presented in Figure 11 on  
 408 the right.

Symbol	Name	Unit
$\underline{E}_T(t)$	evapotranspiration	$[ET^{-1}L^{-2}]$
$\underline{H}(t)$	thermal convective flux	$[EL^{-2}T^{-1}]$
$\underline{J}(t)$	precipitation rate	$[ET^{-1}L^{-2}]$
$\underline{J}_g$	thermal conduction losses to the ground	$[ET^{-1}L^{-2}]$
$\underline{Q}_g(t)$	discharge	$[ET^{-1}L^{-2}]$
$\underline{R}_n(t)$	Net Radiation	$[EL^{-2}T^{-1}]$
$U_g(t)$	internal energy storage per unit area	$[EL^{-2}]$

409 Furthermore, hydraulic conductivity,  $K_S$ , is thought to control the water flux,  $Q_G$ ,  
 410 while the Leaf Area Index (LAI) controls evapotranspiration and radiation response of  
 411 the system (through long wave radiation fluxes). Admittedly, some simplification have  
 412 been made when coupling the water budget with the energy budget, however, the pro-  
 413 cedure is quite general and can be used for more complicated cases.



415 **Figure 12.** The simple vegetation growth model presented in Montaldo et al. (2005). It con-  
 416 sists of three coupled ODEs, which account for aboveground, below ground and dead vegetation.

414 **6.2 Carbon budget**

The interactions of water budget with the ecosystem can also be represented with EPN. As an example, we use a simple vegetation growth model presented in Montaldo et al. (2005) and further developed in Della Chiesa et al. (2014). The model consists of three ODEs, for above ground vegetation,  $B_g$ , roots,  $B_r$ , and dead material,  $B_d$ :

$$\frac{dB_g}{dt} = a_a P_g + T_{ra} - R_g - S_g \quad (13)$$

where  $B_g$  is the mass of the green aboveground biomass,  $P_g$  is the gross photosynthesis,  $a_a$  is the allocation partition coefficient to shoots,  $T_{ra}$  is the translocation of carbohydrates from the roots to the living aboveground biomass,  $R_g$  is the respiration of the aboveground biomass, and  $S_g$  the senescence of the aboveground biomass.

$$\frac{dB_r}{dt} = a_r P_g - T_{ra} - R_r - S_r \quad (14)$$

where  $B_r$  is the living root biomass,  $a_r$  ( $a_r + a_a = 1$ ) is the allocation partition coefficient to roots,  $R_r$  is the respiration from roots,  $S_r$  the senescence of roots.

$$\frac{dB_d}{dt} = S_g - L_a \quad (15)$$

420 where  $B_d$  are the standing dead,  $S_g$  is the senescence of aboveground biomass and  $L_A$   
 421 is the litter fall. All of these quantities are described in the dictionary in Table 6 and  
 are represented by the EPN in Figure 12. This model is presented to show how vegeta-

417 **Table 6.** Dictionary relative to the model of vegetation growth in Montaldo et al. (2005) and  
 418 illustrated in Figure 12.

Symbol	Name	Type	Unit
$a_a$	allocation partition coefficient for aboveground biomass	P	[-]
$a_r$	allocation partition coefficient for root compartments	P	[-]
$B_d$	standing dead biomass	SV	[M L <sup>-2</sup> ]
$B_g$	green aboveground biomass	SV	[M L <sup>-2</sup> ]
$B_r$	living root biomass	SV	[M L <sup>-2</sup> ]
$L_a$	litter fall	F	[M L <sup>-2</sup> T <sup>-1</sup> ]
$P_g$	gross photosynthesis	F	[M L <sup>-2</sup> T <sup>-1</sup> ]
$R_g$	transpiration from aboveground biomass	F	[M L <sup>-2</sup> T <sup>-1</sup> ]
$R_r$	transpiration from root biomass	F	[M L <sup>-2</sup> T <sup>-1</sup> ]
$S_g$	senescence of the aboveground biomass	F	[M L <sup>-2</sup> T <sup>-1</sup> ]
$S_r$	senescence of the root biomass	F	[M L <sup>-2</sup> T <sup>-1</sup> ]
$T_{ra}$	translocation of carbohydrates from roots to the aboveground biomass	F	[M L <sup>-2</sup> T <sup>-1</sup> ]

422 tion can interact with the hydrological cycle, an aspect that can be fully revealed only  
 423 through an expression table. For the sake of simplicity, Table 7 does not contain the com-  
 424 plete mathematical expressions, which are fully discussed in Della Chiesa et al. (2014);  
 425 Montaldo et al. (2005), but it does provide the variable dependence needed to produce  
 426 the h-connections between the vegetation model and the water and energy budgets. The

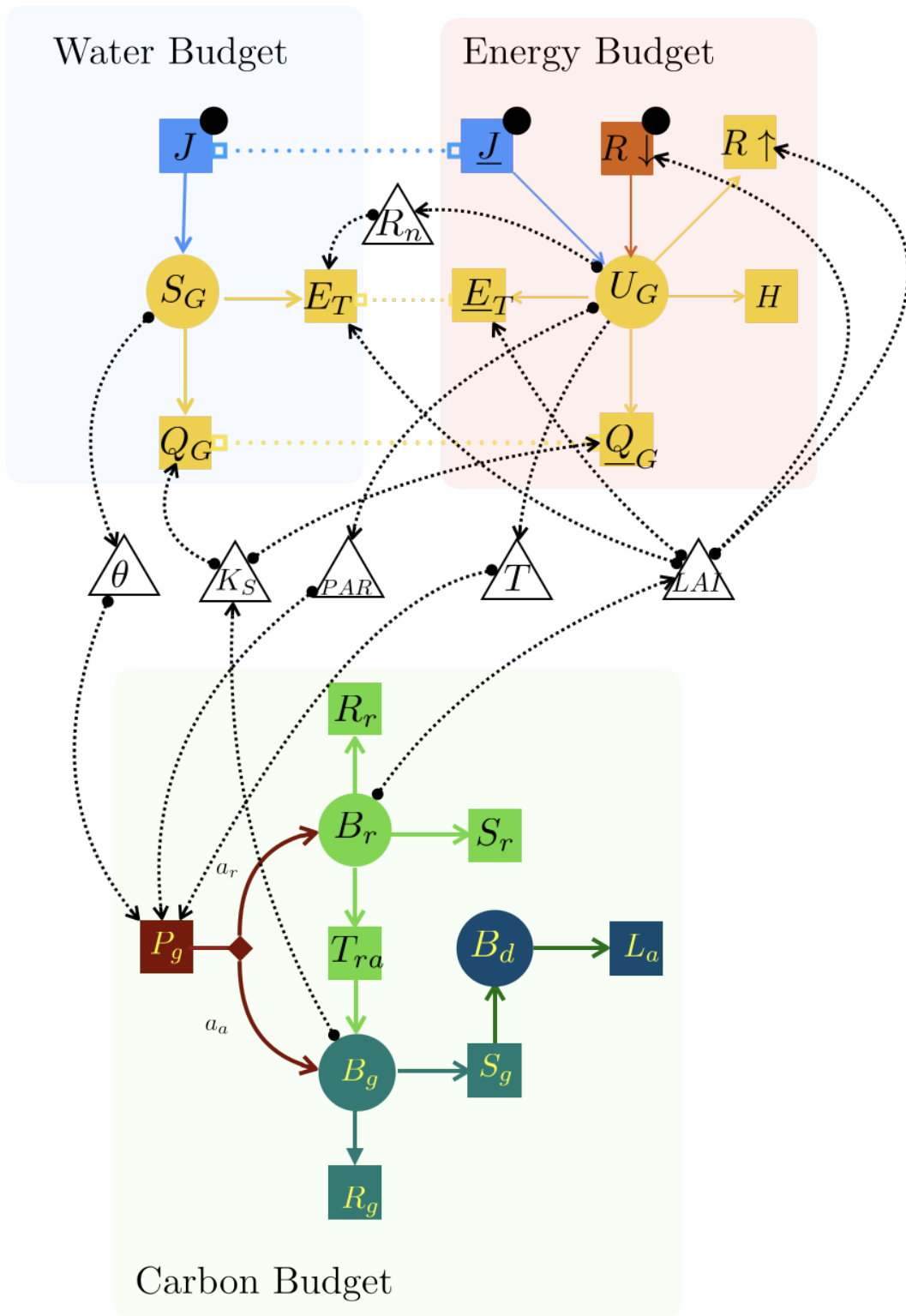
419 **Table 7.** Expression Table relative to the model of vegetation growth in Figure 13.

Symbol	Name	Expression
$P_g$	gross photosynthesis	$P_g(\Delta CO_2, r_a, r_c)$

427 interesting fact is that, through parameters like the  $LAI$ , the aboveground vegetation  
 428 controls evapotranspiration and radiation, while roots are thought to control the hydraulic  
 429 conductivity,  $K_S$ . Photosynthesis feeds a vegetation system and is controlled by vari-  
 430 ables such as temperature,  $T$ , photosynthetic active radiation (here made dependent on  
 431 the energy budget), and soil water content,  $\theta$ . All of this is represented in Figure 13 and  
 432 is discussed in the next section.  
 433

## 434 7 Discussion

435 While the graphs of the water budget, energy budget and vegetation growth are  
 436 themselves direct, acyclic graphs, the whole coupled graph, inclusive of h-wiring, shows  
 437 loops, like the one between  $U_G \rightarrow T \rightarrow P_g \rightarrow B_r \rightarrow LAI \rightarrow R \downarrow \rightarrow U_G$ , that depict a  
 438 feedback. Therefore, to really understand the interactions between the three dynamical  
 439 systems graphically, we have to use h-wiring as we do in Figure 13. Notably, while  
 440 the water budget can be represented with traditional reservoirs, the traditional graphics  
 441 fall short in representing the other budgets.



442 **Figure 13.** Representation of the water and energy budgets coupled with the vegetation  
 443 dynamic model. The coupling happens entirely through h-wiring

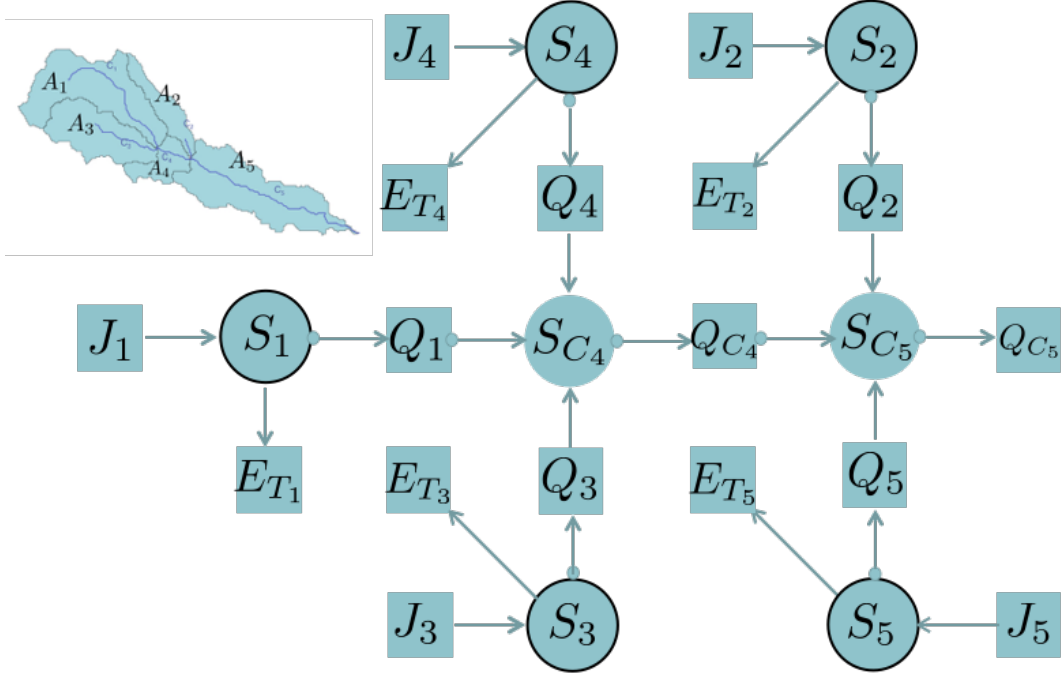
Figure 13 is only for demonstration purposes and, as such, the connections shown are hypothetical. As we have not implemented and tested such a model, the relations presented are based on educated guesses. The quantities that appear in the h-wiring network are constraints on the dynamical model parameters and work as valves that regulate the fluxes. Without h-wiring, the connections between sub-models are not evident. Although, the flux connections (f-wiring) alone are sufficient to write the correct ODEs in their completeness, including feedback loops, once complemented by the appropriate expression tables. When H. G. Savenije and Hrachowitz (2017) write, “The most important active agent in catchments is the ecosystem. [...]. Ecosystems do this in the most efficient way, establishing a continuous, ever-evolving feedback loop with the landscape and climatic drivers”, they refer to the ability of ecosystems, represented in Figure 13 by the bottom set of ODEs, to control the water cycle. The Figure shows how this happens through the action of controllers that link vegetation to both the water and energy cycles. We do not know yet if the system devised includes the right properties to obtain the dynamical richness desired. To get an answer one should look towards system and control theories. These (Kalman, 1959) offer more than fifty years’ worth of literature to help deal properly with interacting systems. In fact, one pivotal concept in system and control theories is **controllability**, i.e. the possibility that a system that has drifted into an undesirable state can be steered back to another desirable one. Linear theory (Willems, 2007) contains theorems and tools (Luenberger, 1979; Kalilath, 1980; Sontag, 1998) that can assess controllability precisely but, unfortunately, our HDSys is not linear and, at first sight, our controllers do not seem to fit the concept of **actuators**, the agents that perform the control.

To treat non-linearities more completely, more sophisticated analyses are needed, (Liu & Barabasi, 2016). Fortunately, a lot has been accomplished since the 1970s (Haynes & Hermes, 1970; Hermann & Krener, 1977; Cornelius & Kath, 2013). Great strides have been made, both from an analytical point of view and from a graph theory point of view, (Yamada & Foulds, 1990; Liu & Barabasi, 2016). Notably, the latter results are directly interpretable by using the EPN presented here, though an exploitation of these possibilities goes beyond the scopes of this paper. However, it should be noted that any graphical representation that does not contain fluxes in explicit form (i.e. as nodes of the graphs) and h-wiring, brings to a scanty graphical representations of the dynamics and, as a consequence, to incorrect graphical analyses.

The discussion so far has been referred to a single spatial unit or HRU. If a catchment is divided into various parts, the EPN of the single spatial units can be joined to obtain the integral distributed view of the basin. For illustrative purposes, in this paper we use a simple catchment partition based on the identification of subcatchments, as shown in Figure 14.

In the example case, the basin is subdivided in 5 HRUs (Figure 14, top left), which have been derived by dividing the river network into five links  $C_1$  to  $C_5$ . It is assumed that the external fluxes to the HRU are rainfall  $J_i$  in input, and evapotranspiration  $E_{T_i}$  and discharges  $Q_i$  ( $i \in \{1, \dots, 5\}$ ) in output. Each HRU flows into a channel stream, for instance, the HRU of area  $A_4$  flows into  $C_4$  and subsequently to  $C_5$ . The complete network of interactions can be represented as in Figure 14. A black frame marking some of the external places indicates that they are actually *compound places*. These can be expanded by using embedded models, like those shown in the Figures of the previous sections or some generalization of the more complex model of Figure 13. The HBV model (Seibert & Vis, 2012) is meant to be just such a model: the HBV structure presented in Figures 2 and 8 can be used for any sub-catchment of the basin analyzed.

Figure 14 exploits the compositionality of EPN and shows how it can be used to represent any river network. Semi-distributed modeling can become very complex and even have heterogeneous elements in each compound node. It is not a matter for this paper to discuss when it becomes too complicated to be reasonably useful. The scopes of



493 **Figure 14.** A small river networks with 5 HRUs (top left) and the corresponding EPN. There  
 494 is a black frame marking some of the places to indicate that they are compound places; these  
 495 should be expanded to reveal the full structure of the system.

500 our representation is to make the model structures presented as clear as possible and,  
 501 eventually, to exemplify it. To pursue the latter task, it is helpful to translate the graphs  
 502 into mathematics, as we do in the next section.

## 503 8 A formal mathematical treatment of EPN

504 So far we have treated the graphics and their relation to mathematics in a conversa-  
 505 tional way. However, these relations can be more precisely stated by providing a set  
 506 of definitions for the entities appearing in EPN, which the reader can find below. The  
 507 definitions have the advantage of formalizing the topology of the models by introduc-  
 508 ing appropriate adjacency and incidence matrixes. These matrixes, in turn, reveal that  
 509 the structure of the hydrological dynamical system can be studied objectively using tech-  
 510 niques derived by algebraic topology (Fiedler, 1973) and, as mentioned in the previous  
 511 sections, already used in other fields Our definitions (any item marked with a bullet, ●)  
 512 expand the notation introduced in Navarro-Gutiérrez, Ramírez-Treviño, and Gómez-Gutiérrez  
 513 (2013) and are modified as suggested by Baez and Pollard (2017). To exemplify them,  
 514 we will refer to that part of the HBV model that has been framed in black in Figure 8.

### 515 8.1 The topology of a HDSys

- 516 •  $\mathcal{P} = \{p_1, \dots, p_n\}$  is the set of  $n$  places (reservoirs). In our graphical notation, they  
 517 are identified by  $n$  circles. In the HBV example,  $\mathcal{P} = \{SWE, W_S, S_{soil}\}$ .
- 518 •  $\mathcal{T} = \{t_1, \dots, t_l\}$  is the set of  $l$  transitions (fluxes). Graphically, they are represented  
 519 by  $l$  squares. In the HBV example,  $\mathcal{T} = \{M, R, M_d, F, E_{act}, P\}$



520 In EPN the relationships between these two types of nodes (i.e. places and transitions)  
 521 can be expressed with two incidence matrices.

- 524 •  $A^-$  is the incidence matrix that represents the connections from places to tran-  
 525 sitions, i.e. it is an  $n \times l$  matrix, where the element  $(i, j)$  is marked with 1 if place  
 526  $i$  outputs to transition  $j$  and otherwise it is 0. In our graphical notation the con-  
 527 nections are shown with oriented arcs joining the appropriate couple  $(p_i, t_j)$ . With  
 respect to the HBV example,  $A^-$  is shown in table 8.

	$R$	$M$	$M_d$	$F$	$E_{act}$	$P$
$SWE$	0	1	0	0	0	0
$W_s$	1	0	1	0	0	0
$S_{soil}$	0	0	0	1	1	0

522 **Table 8.**  $A^-$  matrix for the HBV example.  $P$  is an input and has no places connecting to it,  
 523 therefore, its column does not contain any 1s.

- 528 •  $A^+$  is the incidence matrix that represents connections from transitions to places,  
 529 i.e. it is an  $l \times n$  matrix, where the element  $(k, m)$  is marked with 1 if transition  
 530  $k$  is an input to place  $m$ ; otherwise it is 0. Graphically the connections are ori-  
 531 ented arcs joining  $(t_k, p_m)$  for the appropriate  $k$  and  $m$ . The  $A^+$  matrix relative  
 532 to the HBV example is shown in Table 9

	$SWE$	$W_S$	$S_{Soil}$
$R$	1	0	0
$M$	0	1	0
$M_d$	0	0	1
$F$	0	0	0
$E_{act}$	0	0	0
$P$	1	0	1

529 **Table 9.** The  $A^+$  matrix relative to the HBV model.  $F$  and  $E_{act}$  are outputs of the whole  
 530 system and therefore their rows contain only 0s.

535

536 There are two possible products of the incidence matrices,  $A^+$  and  $A^-$ , both of which  
 537 result in a square matrix:

- 540 •  $A = A^- \cdot A^+$  is the  $(n \times n)$  adjacency matrix that identifies the connections be-  
 tween places. The  $A$  matrix for the HBV model is shown below in Table 10

	$SWE$	$W_S$	$S_{Soil}$
$SWE$	0	1	0
$W_S$	1	0	1
$S_{Soil}$	0	0	0

538 **Table 10.** The  $A$  matrix for the HBV example. The anti-diagonal 1s reveal the presence of a  
 539 loop.

- 543 •  $\tilde{A} = A^+ \cdot A^-$  is the  $(l \times l)$  adjacency matrix that identifies the connection between transitions. The  $\tilde{A}$  for the HBV example is presented in Table 11

	$R$	$M$	$M_d$	$F$	$E_{act}$	$P$
$R$	0	1	0	0	0	0
$M$	1	0	1	0	0	0
$M_d$	0	0	0	1	1	0
$F$	0	0	0	0	0	0
$E_{act}$	0	0	0	0	0	0
$P$	0	1	0	1	1	0

541 **Table 11.** The  $\tilde{A}$  adjacency matrix for transitions with respect to the HBV example. It reveals  
542 the connections between fluxes

544

545 Transitions and places, and their relationships as expressed in incidence and ad-  
546 jacency matrices, can be used to represent the ODE system of any budget (mass, energy,  
547 momentum).

548 Starting from any one of the places (circles), transitions (squares) in the graphic  
549 and:

- 550 • following the arcs we get a **causal path**. When two variables are connected by  
551 an arc, the upstream entity is said to cause the downstream one. Therefore a tran-  
552 sition is caused by the upstream place and a place by the upstream fluxes. Causal-  
553 ity is inherited, in that all upstream variables have causal influence on downstream  
554 ones.

555 However, the resulting EPN, do not show the feedbacks between state variables  
556 completely because some of these can be hidden in the flux expressions. Therefore, to  
557 provide a more complete visual representation of the causal relationships between vari-  
558 ables, we have introduced the concept of controllers. Controllers are a function of a state  
559 variable (originated in a place) that contribute in the flux expressions of one or more tran-  
560 sitions. They are explicitly represented by triangles in the graph. A rectangular incidence  
561 matrix  $B$ , of dimensions  $(n \times l)$ , indicates the places that are connected to transitions  
562 via controllers. The resulting web of interactions is called hidden wiring or **h-wiring**.  
563  $B$  can be split into two matrices (as was the case for  $A$ ).

564 If:

- 565 •  $\mathcal{C} = \{c_1, \dots, c_m\}$  is the set of controllers. In the HBV example there is just one con-  
566 troller,  $T$ , the temperature, therefore  $\mathcal{C} = \{T\}$ .  
567 •  $B^-$  is the incidence matrix representing the connections from places to controllers.  
568 It is an  $n \times m$  matrix with the non-null element  $(i, j)$  set to 1 if place  $i$  is connected  
569 to controller  $j$ . Graphically, oriented dashed arcs are used to connect circles to tri-  
570 angles. The  $B^-$  matrix of the HBV example is represented in Table 12.  
571 •  $B^+$  is the incidence matrix  $(m \times l)$  between controllers and transitions. Graph-  
572 ically the connection between controllers and transitions are represented by ori-  
573 ented dashed arcs between triangles and squares. The usual example from the HBV  
574 model reads as in Table 13.  
575  
576

577 Then:

	$T$
$SWE$	0
$W_s$	0
$S_{Soil}$	1

567 **Table 12.** Matrix of the connections between places and controllers in the HBV example.

	$R$	$M$	$M_d$	$F$	$E_{act}$	$P$
$T$	1	1	0	0	1	1

572 **Table 13.**  $B^+$  matrix relative to the HBV example.

- 580
- the incidence matrix describing h-wiring is  $B = B^- \cdot B^+$ ;  $B$  for the HBV example is shown in Table 14.

	$R$	$M$	$M_d$	$F$	$E_{act}$	$P$
$SWE$	0	0	0	0	0	0
$W_s$	0	0	0	0	0	0
$S_{Soil}$	1	1	0	0	1	1

578 **Table 14.** Incidence matrix between the places and transition generated by h-wiring in the  
579 HBV example.

- 581
- the adjacency matrix  $C = B^- \cdot B^+ \cdot A^+$  describes the h-connections between places (via flux controllers). This adjacency matrix is shown in Table 15 with respect to the HBV example. Unlike the other adjacency and incidence matrixes, there are 2 connections between  $S_{soil}$  and  $SWE$ , due to the multiple arrows exiting from  $T$ . Also interesting is the self-loop for  $S_{Soil}$  through precipitation separation, since temperature is thought to be affected by soil water quantity. We note here that this feedback is not contained in the HBV model; it is introduced here only for illustrative purposes.

	$SWE$	$W_s$	$S_{Soil}$
$SWE$	0	0	0
$W_s$	0	0	0
$S_{Soil}$	2	1	1

582 **Table 15.** Adjacency matrix  $C$  for the HBV example.

- 590
- The total adjacency matrix  $D := A + C$  contains all the connections between places, both with and without controllers.  $D$  for the HBV example is shown in Table 16. The h-wiring introduces feedback between  $S_{soil}$  and  $W_s$ , which was not apparent without it.

597 Therefore, to define EPN and its information, we need a 7-tuple:

- 598
- $\mathcal{X} = (\mathcal{P}, \mathcal{T}, \mathcal{C}, A^-, A^+, B^-, B^+)$ , respectively representing: places, transitions, controllers, incidence matrix from places to transitions, from transitions to places, from
- 599

	$SWE$	$W_s$	$S_{Soil}$
$SWE$	0	1	0
$W_s$	1	0	1
$S_{Soil}$	2	1	1

591 **Table 16.** The  $D$  matrix for the HBV example. It represents all the connections between  
 592 places, either mediated by fluxes or by h-wiring.

600 places to controllers, and from controllers to transitions, that we call the **topol-**  
 601 **ogy** of the EPN.

602 Models with the same topology can have different fluxes and state variables.

### 603 8.2 The semantics of a HDSys

604 The **semantics** provide all the information needed to complete the equations of  
 605 a given system on the basis of its topology. Let us define the semantics as follows.

606 Let:

- 607 •  $D$  be the **dictionary** or **lexicon** of a model. It associates each symbol in the topol-  
 608 ogy to its meaning (and other information such as units and the role of the vari-  
 609 able). Various examples were given in the previous sections, such as Tables 1 above  
 610 and Table A.1 below.
- 611 •  $\dot{S}$  be the set of expressions for places, associating to each place its mathematical  
 612 operator (in this paper the default expression for a place is the time derivative of  
 613 the state variable);
- 614 •  $E$  be the set of expressions for fluxes, associating to each flux its algebraic form.  
 615 Examples are given in Tables 2 and B;
- 616 •  $C$  be the set of expressions that define controllers as functions of state variables.  
 617 Table B3 is an example for the Ard-Burn example.

618 Then,

- 619 • the **semantics** of an EPN is the quadruple:  $\mathcal{Y} = (D, E, C, \dot{S})$

620 Finally,

- 621 • The pair  $\mathcal{M} = (\mathcal{X}, \mathcal{Y})$  (topology and semantics) fully defines a HDSys.

### 622 8.3 A definition of hydrological dynamical systems

623 Some further definitions can be useful in understanding the nature of the model  
 624  $\mathcal{M}$ .

625 The set:

- 626 •  $s_i = \{p_j | A_{ji}^- > 0\}$  is said to be the **preset** (or the set of **sources**) of the tran-  
 627 sition  $t_i$ ; In Table 8 this set can be deduced from the non-null terms in the columns.
- 628 •  $o_i = \{p_j | A_{i,j}^+ > 0\}$  is said to be the **postset** or the set of **targets** of transition  
 629  $t_i$ . In Table 9 they are the non-null terms in any row.

630 Then,

- 631 • A system is said to be **open** if there are transitions with both empty presets (rows  
 632 with all zeroes in Table 9) and empty postsets (columns with all zeroes in Table  
 633 8). Otherwise, a system is said to be **closed**. Please note that a topology with empty  
 634 presets but non-empty postsets (or, vice versa, with empty postsets and non-empty  
 635 presets) is dynamically meaningless.

636 Analogously, the same definitions of preset and postset can be used for controllers:

- 637 •  $u_i = \{p_j | B_{ij}^- > 0\}$  is said to be the preset of the controller  $c_i$ ,  
 638 •  $v_i = \{p_j | B_{ij}^+ > 0\}$  is said to be the postset of the controller  $c_i$

639 Therefore, we can conclude that:

- 640 • any open or closed system, as defined above, can be **externally constrained** if  
 641 there are controllers with empty presets.

642 Observing that the set of expressions of fluxes,  $\mathbf{E}$ , is a column (tuple) of symbols  
 643 of length  $l$ , like the transitions to which it is associated, we can build the vectors of ex-  
 644 pressions:

- 645 •  $O = A^- \cdot \mathbf{E}$ , where the element  $O_j$  contains all the output fluxes from place  $j$ ;  
 646 and  
 647 •  $I = \tilde{A}^+ \cdot \mathbf{E}$ , where  $\tilde{A}^+$  is the transpose of the incidence matrix  $A^+$  and the ele-  
 648 ment  $I_j$  contains all the inputs to place  $j$ .

Applying these definitions, any HDSys can be written as:

$$\dot{\mathbf{S}} = (\tilde{A}^+ - A^-) \cdot \mathbf{E} = I - O \quad (16)$$

where  $\dot{\mathbf{S}}$  is the tuple of differential operators acting on place variables. This can be ex-  
 pressed in terms of the components:

$$\frac{dS_j}{dt} = ((\tilde{A}^+ - A^-) \cdot \mathbf{E})_j = \tilde{A}_{ji}^+ \mathbf{E}_i - A_{ji}^- \mathbf{E}_i = I_j - O_j \quad (17)$$

649 where, the substitution  $S_j \rightarrow \frac{dS_j}{dt}$  has been assumed for all the state variables in  $\dot{\mathbf{S}}$  and  
 650 the sum of all the transitions that connect to the place  $j$  is implicit in the tuple prod-  
 651 uct.

#### 652 8.4 Composition of models and feedbacks

653 Models are compositional in the sense that, given two model  $\mathcal{M}$  and  $\mathcal{M}'$ , we say  
 654 that

- 655 •  $\mathcal{M}$  and  $\mathcal{M}'$  can be composed if at least one output of one model coincides with  
 656 one input of the other.

657 However, models can also be composed by sharing controllers. For instance, a model of  
 658 the energy budget can provide the temperature  $T$ , which is a controller of the model HBV.  
 659 Thence, the energy budget not only constrains the behavior of *HBV* but can also be com-  
 660 posed with it. We can say that, given two models  $\mathcal{M}$  and  $\mathcal{M}'$ , they can be composed:

- 661 • by sharing fluxes (**f-wiring**); or  
 662 • by sharing controllers (**h-wiring**)

663 This means that our models, and their representations, have at least two associative prop-  
 664 erties that can be used to obtain arbitrarily complicated models. The use of h-wiring is

665 only fully possible with a Petri net type of representation because in other graphical sys-  
 666 tems, fluxes (transitions) do not have the graphical status of nodes.

## 667 9 Conclusions

668 In this paper we introduced an extension of Petri Nets to describe lumped hydro-  
 669 logical models and make evident that they are part of the great family of dynamical sys-  
 670 tems and/or compartmental models. The EPN representation:

- 671 • is adequate to describe any lumped hydrological system and the interactions be-  
 672 tween the hydrological, energy and carbon cycles, which form the basis for the mod-  
 673 elling of Earth system interactions.
- 674 • standardizes the way to represent hydrological models and interactions;
- 675 • streamlines the process of documenting hydrological models;
- 676 • facilitates user comprehension of eco-hydrological interactions (number of places  
 677 corresponds to the number of equations, number of transitions to the number of  
 678 fluxes, and number of controllers to the number of constraints imposed on the fluxes);
- 679 • can be used to organize process interactions hierarchically, even when the math-  
 680 ematical flux expressions are not set;
- 681 • allows for an easy comparison of model structures in terms of topology and seman-  
 682 tics (via specific expression of fluxes and constraints);
- 683 • visually represents feedback loops between subcomponents, even those implied by  
 684 non-linear terms, that are hidden in other treatments of the subject;
- 685 • provides a complete visual representation of the causal relation between variables  
 686 used in models;
- 687 • helps to understand lumped models as systems of systems of ODEs that can be  
 688 composed to form larger systems;
- 689 • builds a bridge with analysis techniques developed in mathematics or other dis-  
 690 ciplines, such as theoretical biology, neuroscience and computer science;
- 691 • hints how results from linear and non-linear Systems and Control theory can be  
 692 used to gain insight into hydrological processes and evaluate the control exerted  
 693 by ecosystems on hydrology and by hydrology on ecosystems.

694 At the same time, being general, EPN can be easily used in other disciplines, such as ecol-  
 695 ogy, chemistry, biology and population dynamics.

696 **A Dictionaries and Expression table for the HBV model**

697 In this Appendix we report the Dictionary and the Expression table for the HBV  
 698 model. The information presented, together with the EPN, allows one to write the dy-  
 699 namical system that corresponds to the HBV model with confidence.

700 **Table A.1.** Dictionary for the HBV model Seibert and Vis (2012). *P* type stands for “parame-  
 701 ter”; *F* for “flux”; *SV* for “state variable”; *C* for controller; *V* for independent variable

Symbol	Name	Type	Units
$E_{act}$	actual evapotranspiration	F	[L T <sup>-1</sup> ]
$E_{pot}$	potential evapotranspiration	F	[L T <sup>-1</sup> ]
$E_{POT,M}$	long term mean potential evapotranspiration	P	[L T <sup>-1</sup> ]
$F(t)$	flux of water to the upper reservoir	F	[L T <sup>-1</sup> ]
$M$	rate of snow melting	F	[L T <sup>-1</sup> ]
$M_d$	release of liquid water from snow	F	[L T <sup>-1</sup> ]
$P^\bullet$	precipitation	F	[L T <sup>-1</sup> ]
$P_{BETA}$	exponent in flux to upper zone	P	[-]
$P_{CFMAX}$	degree-day factor in snow melting	P	[L T <sup>-1</sup> ]
$P_{CFR}$	proportion of water refreezing	P	[-]
$P_{CET}$	parameter in defining $E_{POT}$	P	[T-1]
$P_{FC}$	maximum value of soil storage	P	[L]
$P_{K0}$	parameter in estimation of flux out of upper zone	P	[T <sup>-1</sup> ]
$P_{K1}$	parameter in estimation of flux out of upper zone	P	[T <sup>-1</sup> ]
$P_{K2}$	parameter in estimation of flux out of LZ	P	[T <sup>-1</sup> ]
$P_{LT}$	parameter: entering in evaporation estimation	P	[-]
$P_{perc}$	percolation to groundwater	F	[L T <sup>-1</sup> ]
$P_{MAXBAS}$	parameter: in definition of $c(i)$	P	[-]
$P_{TT}$	threshold parameter for melting activation	P	[T]
$Q_{GW1}$	runoff from the upper zone to the surface waters	F	[L T <sup>-1</sup> ]
$Q_{GW2}$	groundwater flow	F	[L T <sup>-1</sup> ]
$Q_{sim}$	river network discharge	F	[L T <sup>-1</sup> ]
$R$	rate of liquid water refreezing	F	[L T <sup>-1</sup> ]
$S_{soil}$	water in soil/root zone	SV	[L]
$S_{LZ}$	groundwater storage	SV	[L]
$S_R$	runoff storage	SV	[L]
$S_{UZ}$	water Storage in the upper zone	SV	[L]
$SWE$	Snow Water Equivalent	SV	[L]
$T^\bullet$	temperature	C	[T]
$T_M$	long-term average temperature	P	[T]
$W_S$	liquid water in snow	SV	[L]

704 The expressions in Table A.2 are quite long, given our desire to respect the names  
 705 used in the paper Seibert and Vis (2012); we are forced, therefore, to introduce the an-  
 706 cillary table A.3 that contains the missing sub-expressions. Once sub-expressions are sub-  
 707 stituted into their corresponding variable, the complete form of the fluxes is obtained.

709 **B Dictionary and Expression table for the Loch Ard-Burn model**

710 Here we present the dictionary and the expression table for the Loch Ard-Burn model.  
 711 Notwithstanding the apparent simplicity of Figure 3, the model becomes quite compli-  
 712 cated when complete information is provided.



702 **Table A.2.** Expression table for HBV model. The flux expressions are quite long and, there-  
703 fore, some ancillary quantities are defined in table A.3

Flux	Name	Expression
$E_{act}$	actual evapotranspiration	$E_{pot} \min \left( \frac{S_{soil}(t)}{P_{FC} P_{LT}}, 1 \right)$
$F(t)$	flux of water to the upper reservoir	$I(t) \left( \frac{S_{soil}}{P_{FC}} \right)^{P_{BETA}}$
M	rate of snow melting	$P_{CFMAX}(T(t) - P_{TT})$
$M_d$	release of liquid water from snow	$M - R$
$P$	precipitation	•
$P_{perc}$	percolation to groundwater	
$Q_{GW1}$	runoff from the upper zone to the surface waters	$P_{K2} S_{LZ}$
$Q_{GW2}$	groundwater flow	$P_{K0} \max(S_{UZ} - P_{UZL}, 0) + P_{K1} S_{UZ}$
$Q_{sim}$	river network discharge	$\sum_{i=1}^{P_{MAXBAS}} c(i)(Q_{GW1}(t - i + 1) + Q_{GW2}(t - i + 1))$
$R$	rate of liquid water refreezing	$P_{CFR} P_{CFMAX}(P_{TT} - T(t))$

708 **Table A.3.** Table of ancillary variables in the HBV model Expression Table

Variable	Name	Expression
$c(i)$	ancillary variable in $Q_{sim}$	$\int_{i-1}^i \frac{2}{P_{MAXBAS}} - \left  u - \frac{P_{MAXBAS}}{2} \right  \frac{4}{P_{MAXBAS}^2} du$
$E_{pot}$	potential evapotranspiration	$(1 + P_{CET}(T(t) - T_M)) E_{pot,M}$
$I(t)$	sum of snow melt and precipitation	$S_{soil} + M_D$

713 **Table B.1.** Dictionary for the Loch Ard-Burn model. Most of the nomenclature derives from  
714 (Hrachowitz et al., 2013). However, in that paper, the  $S_O$  reservoir is not drawn and, in our opin-  
715 ion, some symbols were not named properly; the underlined words represent more appropriate  
716 names, in our opinion.

Symbol	Name	Type	Units
$C_E$	partition coefficient between evapotranspirations	C	[-]
$C_R$	partition coefficients between runoff types	P	[-]
$E_p$	potential Evapotranspiration	F	[L T <sup>-1</sup> ]
$E_{SI}$	evaporation from vegetation	F	[L T <sup>-1</sup> ]
$E_{SU}$	transpiration from unsaturated reservoir	F	[L T <sup>-1</sup> ]
$E_{SF}$	transpiration from fast responding reservoir	F	[L T <sup>-1</sup> ]
$h_F$	response time distribution for $X_F$ reservoir	[]	[T <sup>-1</sup> ]
$h_S$	response time distribution for $X_S$ reservoir	[]	[T <sup>-1</sup> ]
$K_F$	storage coefficient of fast reservoir	P	[T <sup>-1</sup> ]
$K_S$	storage coefficient of slow reservoir	P	[T <sup>-1</sup> ]
$I_{max}$	maximum interception	P	[L]
$L_p$	transpiration threshold	P	[-]
$P_{max}$	percolation capacity	P	[L T <sup>-1</sup> ]
$P_R^\bullet$	rainfall	F	[L T <sup>-1</sup> ]
$P_{TF}$	throughfall	F	[L T <sup>-1</sup> ]
$Q_{SF}$	runoff from fast reservoir	F	[L T <sup>-1</sup> ]
$Q_{OF}$	overland flow	F	[L T <sup>-1</sup> ]
$Q_{SS}$	runoff from slow reservoir	F	[L T <sup>-1</sup> ]
$R_F$	recharge of fast reservoir	F	[L T <sup>-1</sup> ]
$R_O$	flux from hidden old water reservoir to unsaturated zone	F	[L T <sup>-1</sup> ]

Symbol	Name	Type	Units
$R_P$	preferential recharge of slow reservoir	F	[L T <sup>-1</sup> ]
$R_S$	recharge of <u>old water</u> reservoir	F	[L] T <sup>-1</sup>
$R_U$	<u>percolation from the unsaturated reservoir</u>	F	[L T <sup>-1</sup> ]
$S_I$	intercepted storage	SV	[L]
$S_O$	passive storage in old water reservoir	SV	[L]
$S_S$	storage in slow reservoir	SV	[L]
$S_U$	storage in unsaturated reservoir	SV	[L]
$S_{U_{max}}$	storage capacity in unsaturated reservoir	P	[L]
$T_F$	<u>concentration time</u> for fast reservoir	P	[T]
$T_S$	<u>concentration time</u> for slow reservoir	P	[T]
$X_F$	reservoir creating lag time between $S_U \rightarrow S_F$	SV	[L]
$X_S$	reservoir creating lag time between $S_U \rightarrow S_S$	SV	[L]
$\beta$	shape parameter	P	[-]

717 **Table B.2.** Expression table for the Loch Ard-Burn model. It contains expressions for all the  
 718 fluxes. It requires an ancillary table for all the new definitions included in the expressions.

Variable	Name	Expression
$E_{SI}$	evaporation from vegetation	$\min(S_I/dt, E_p)$
$E_{SU}$	transpiration from unsaturated reservoir	$E_p C_E \min(1, S_U/(S_{U_{max}} L_p))$
$E_{SF}$	transpiration from fast responding reservoir	$\min(E_p(1 - C_E), S_F/dt)$
$P_R$	Rainfall	•
$P_{TF}$	throughfall	$P_R - \min((I_{max} - S_I)/dt)$
$Q_{SF}$	runoff from fast reservoir	$K_F S_F$
$Q_{OF}$	overland flow	$\max(S_F - S_{F_{max}}, 0)$
$Q_{SS}$	runoff from slow reservoir	$K_S S_S$
$R_F$	recharge of fast reservoir	$C_R(1 - C_p)P_{TF}$
$R_F^*$	delayed flux from fast reservoir	$R_F \star h_F$
$R_O$	flux from hidden old water reservoir to unsaturated zone	$\equiv R_S$
$R_P$	preferential recharge of slow reservoir	$C_R C_P C_E$
$R_S$	recharge of <u>old water</u> reservoir	$P_{max}(S_U/S_{U_{max}})$
$R_S^*$	delayed flux from slow reservoir	$R_S \star h_S$
$R_U$	<u>percolation from the unsaturated reservoir</u>	$(1 - C_R)P_E$

719 **Table B.3.** Ancillary variables of the Loch Ard-Burn dictionary introduced by the flux expres-  
 720 sions

Symbol	Name	Expression
$C_R$	coefficient of partition between runoff types	$(1 + \exp(-S_U/S_{U_{max}} + 0.5))^{-1}$
$h_F$	response time distribution for $X_f$ reservoir	$2(t/T_F^2)$ , for $0 < t < T_F$ ; 0 elsewhere
$h_S$	response time distribution for $X_S$ reservoir	$2(t/T_S^2)$ , for $0 < t < T_S$ ; 0 elsewhere

721 **Table B.4.** Controllers table in the Ard Burn model

Symbol	Name	Expression
$C_E$	coefficient of partition between evapotranspirations	$S_U/(S_U + S_F)$
$E_p$	potential evapotranspiration	?

## Acknowledgments

This work was partially supported by the Steep Streams project. All the Authors participated equally all the phases of the research. We do not have used data in our paper. Finally the Authors thank the Associate Editor, Thorsten Wagener, and three anonymous reviewers for their comments that helped to greatly improve this paper.

## References

- Abera, W., Formetta, G., Brocca, L., & Rigon, R. (2017). Modeling the water budget of the upper blue Nile basin using the jgrass-newage model system and satellite data. *Hydrology and Earth System Sciences*, *21*(6), 3145.
- Alla, H., & David, R. (1998). Continuous and hybrid Petri nets. *Journal of Circuits, Systems, and Computers*, *8*(01), 159–188.
- Baez, J. C., & Biamonte, J. (2012). Quantum techniques for stochastic mechanics. *arXiv preprint arXiv:1209.3632*.
- Baez, J. C., & Pollard, B. S. (2017). A compositional framework for reaction networks. *Reviews in Mathematical Physics*, *29*(09), 1750028.
- Berthomieu, B., & Diaz, M. (1991). Modeling and verification of time dependent systems using time Petri nets. *IEEE transactions on software engineering*, *17*(3), 259–273.
- Beven, K. J. (2011). *Rainfall-runoff modelling: the primer*. John Wiley & Sons.
- Birkel, C., Soulsby, C., & Tetzlaff, D. (2011). Modelling catchment-scale water storage dynamics: reconciling dynamic storage with tracer-inferred passive storage. *Hydrological Processes*, *25*(25), 3924–3936.
- Butts, M. B., Payne, J. T., Kristensen, M., & Madsen, H. (2004). An evaluation of the impact of model structure on hydrological modelling uncertainty for streamflow simulation. *Journal of Hydrology*, *298*, 242–266. Retrieved from <http://doi.org/10.1016/j.jhydrol.2004.03.042>
- Carrera, J., Holzbecher, E., Bonell, M., & Vasiliev, O. F. (2005). Systems approach: the nature of coupled models. In A. Brontstert, B. Kabat, J. Carrera, & S. Ltkemeier (Eds.), *Coupled models of the hydrological cycle* (p. 75–164). Springer.
- Champagnat, R., Esteban, P., Pingaud, H., & Valette, R. (1998). Modeling and simulation of a hybrid system through pr/tr pn-dae model. In *Adpm* (Vol. 98, pp. 131–137).
- Clark, M. P., Nijssen, B., Lundquist, J. D., Kavetski, D., Rupp, D. E., Woods, R. A., ... Rasmussen, R. (2015). A unified approach for process-based hydrologic modeling: 1. modeling concept. *Water Resources Research*, *51*(4), 2498–2514. Retrieved from <http://doi.org/10.1002/2015WR017198>
- Clark, M. P., Slater, A. G., Rupp, D. E., Woods, R. A., Vrugt, J. A., Gupta, H. V., ... Lauren, E. H. (2008). Framework for understanding structural errors (fuse): A modular framework to diagnose differences between hydrological models. *Water Resources Research*, *44*, 1–14. Retrieved from <http://doi.org/10.1029/2007WR006735>
- Cornelius, S. P., & Kath, A. E., W. L. and Motter. (2013). Realistic control of network dynamics. *Nature Communications*, *4*, 1942.
- Della Chiesa, S., Bertoldi, G., Niedrist, G., Obojes, N., Endrizzi, S., Albertson, J., ... Tappeiner, U. (2014). Modelling changes in grassland hydrological cycling along an elevational gradient in the alps. *ecohydrology*, *7*, 1453–1473. doi: 10.1002/eco.1471
- Fenicia, F., & Kavetski, H. H. G., D. and Savenije. (2011). Elements of a flexible approach for conceptual hydrological modeling: 1. motivation and theoretical development. *Water Resources Research*, *47*(11), W11510,1–13. Retrieved from <http://doi.org/10.1029/2010WR010174>

- 774 Fenicia, F., Savenije, H. H., Matgen, P., & Pfister, L. (2008). Understanding catch-  
 775 ment behavior through stepwise model concept improvement. *Water Resources*  
 776 *Research*, 44(1).
- 777 Fenicia, F., Wrede, S., Kavetski, D., Pfister, L., Hoffmann, L., Savenije, H. H. G.,  
 778 & McDonnell, J. J. (2010). Assessing the impact of mixing assumptions on  
 779 the estimation of streamwater mean residence time. *Hydrological Processes*,  
 780 24(12), 1730-1741. Retrieved from <http://doi.org/10.1002/hyp.7595>
- 781 Fiedler, M. (1973). Algebraic connectivity of graphs. *Czechoslovak mathematical*  
 782 *journal*, 23(2), 298-305.
- 783 Gabrielli, C. P., Morgenstern, U., Stewart, M. K., & McDonnell, J. J. (2018). Con-  
 784 trasting groundwater and streamflow ages at the maimai watershed. *Water*  
 785 *Resources Research*, 54(6), 3937-3957. Retrieved from [http://doi.org/](http://doi.org/10.1029/2017WR021825)  
 786 [10.1029/2017WR021825](http://doi.org/10.1029/2017WR021825)
- 787 Gilbert, D., & Heiner, M. (2006). From petri nets to differential equations - an inte-  
 788 grative approach for biochemical network analysis. In S. Donatelli & P. S. Thi-  
 789 agarajan (Eds.), *Proc. icatpn 2006* (p. 181-200). Springer.
- 790 Haas, P. J. (2006). *Stochastic petri nets: Modelling, stability, simulation*. Springer  
 791 Science & Business Media.
- 792 Haynes, G., & Hermes, H. (1970). Nonlinear controllability via lie theory. *SIAM J.*  
 793 *Control*, 8, 450-460.
- 794 Herajy, M., & Heiner, M. (2015). Modeling and simulation of multi-scale environ-  
 795 mental systems with generalized hybrid petri nets. *Frontiers in Environmen-*  
 796 *tal Sciences - Methods*, 3, 53, 1-14. Retrieved from [doi:10.3389/fenvs.2015](https://doi.org/10.3389/fenvs.2015.00053)  
 797 [.00053](https://doi.org/10.3389/fenvs.2015.00053)
- 798 Hermann, R., & Krener, A. (1977). Non linear controllability and observability.  
 799 *IEEE Trans. Automat. Contr.*, 22, 728-740.
- 800 Hrachowitz, M., Savenije, H., Bogaard, T., Soulsby, C., & Tetzlaff, D. (2013). What  
 801 can flux tracking teach us about water age distribution patterns and their  
 802 temporal dynamics? *Hydrology and Earth System Sciences*, 17(2), 2013.
- 803 Jensen, K., & Kristensen, L. M. (2009). *Coloured petri nets: modelling and valida-*  
 804 *tion of concurrent systems*. Springer Science & Business Media.
- 805 Kaiser, D. (2005). Physics and feynman's diagrams. *American Scientist*, 93,  
 806 156,165.
- 807 Kalilath, T. (1980). *Linear systems*. Prentice-Hall.
- 808 Kalman, R. (1959). On the general theory of control systems. *IRE Transactions on*  
 809 *Automatic Control*, 4(3), 481-493.
- 810 Kampf, S., & Burges, S. (2007). A framework for classifying and comparing dis-  
 811 tributed hillslope and catchment hydrologic models. *Water Resources Re-*  
 812 *search*, 43(5), 1-24. Retrieved from <http://doi.org/10.1029/2006WR005370>
- 813 Kirchner, J. (2016). Aggregation in environmental systems -part2: Catchment mean  
 814 transit times and young water fractions under hydrologic nonstationarity. *Hy-*  
 815 *drology and Earth System Sciences*, 20(1), 299-328. Retrieved from [http://](http://doi.org/10.5194/hess-20-299-2016)  
 816 [doi.org/10.5194/hess-20-299-2016](http://doi.org/10.5194/hess-20-299-2016)
- 817 Knoblen, W. J. M., Freer, J., Fowler, K. J. A., Peel, M. C., & Woods, R. A.  
 818 (2019). Modular assessment of rainfall-runoff models toolbox (marmot)  
 819 v1.0: an open source, extendable framework providing implementations  
 820 of 46 conceptual hydrologic models as a continuous space-state formula-  
 821 tions. *Geoscientific Model DEvelopment Discussion*, 1-26. Retrieved from  
 822 <http://doi.org/10.5281/zenodo.2482542>
- 823 Koch, I. (2010). Petri nets—a mathematical formalism to analyze chemical reaction  
 824 networks. *Molecular Informatics*, 29(12), 838-843.
- 825 Koch, I., Reising, W., & Schreiber, F. (2010). *Modeling in systems biology: the petri*  
 826 *net approach* (Vol. 16). Springer Science & Business Media.
- 827 Kuppel, S., Tetzlaff, D., Maneta, M. P., & Soulsby, C. (2018). What can we learn  
 828 from multi-data calibration of a process-based ecohydrological model? *Envi-*

- 829 *ronmental Modelling & Software*, 101, 301–316.
- 830 Liu, Y.-Y., & Barabasi, A.-L. (2016). Control principles of complex systems. *Re-*  
 831 *views of Modern Physics*, 88(3), 247–258. Retrieved from [http://doi.org/10](http://doi.org/10.1103/RevModPhys.88.035006)  
 832 [.1103/RevModPhys.88.035006](http://doi.org/10.1103/RevModPhys.88.035006)
- 833 Lohn, J. D., & Colombano, S. P. (1999). A circuit representation technique for auto-  
 834 mated circuit design. *IEEE Transactions on Evolutionary Computation*, 3(3),  
 835 205–219.
- 836 Luenberger, D. (1979). *Introduction to dynamic systems*. John Wiley & Sons, Inc.
- 837 Marsan, M. A., Balbo, G., Conte, G., Donatelli, S., & Franceschinis, G. (1994).  
 838 *Modelling with generalized stochastic petri nets*. John Wiley & Sons, Inc.
- 839 Merlin, P., & Farber, D. (1976). Recoverability of communication protocols–  
 840 implications of a theoretical study. *IEEE transactions on Communications*,  
 841 24(9), 1036–1043.
- 842 Montaldo, N., Rondena, R., Albertson, J., & Mancini, M. (2005). Parsimonious  
 843 modeling of vegetation dynamics for ecohydrologic studies of water- limited  
 844 ecosystems. *Water Resources Research*, 41(10), W10416. Retrieved from  
 845 <http://doi.org/10.1029/2005WR004094>
- 846 Murata, T. (1989). Petri nets: Properties, analysis and applications. *Proceedings of*  
 847 *the IEEE*, 77(4), 541–580.
- 848 Navarro-Gutiérrez, M., Ramírez-Treviño, A., & Gómez-Gutiérrez, D. (2013). Mod-  
 849 elling the behaviour of a class of dynamical systems with continuous petri  
 850 nets. In *Emerging technologies & factory automation (etfa), 2013 iee 18th*  
 851 *conference on* (pp. 1–6).
- 852 Oster, G., Perelson, A., & Katchalsky, A. (1971). Network thermodynamics. *Nature*,  
 853 234, 393–399.
- 854 Patten, B., Higashi, M., & Burns, T. (1990). Trophic dynamics in ecosystem net-  
 855 works: significance of cycles and storage. *Ecological Modelling*, 51, 1–28. Re-  
 856 trieved from [https://doi.org/10.1016/0304-3800\(90\)90055-L](https://doi.org/10.1016/0304-3800(90)90055-L)
- 857 Petri, C. (1966). *Communication with automata* (Unpublished doctoral dissertation).  
 858 University of Bonn.
- 859 Ramchandani, C. (1974). *Analysis of asynchronous concurrent systems by petri nets*  
 860 (Tech. Rep.). Massachusetts Inst. of Tech Cambridge project MAC.
- 861 Savenije, H. G., & Hrachowitz, M. (2017). Hess opinions catchments as meta-  
 862 organisms a new blueprint for hydrological modelling. *Hydrology and Earth*  
 863 *System Science*, 21, 1107–1116. Retrieved from [https://www.hydrol-earth](https://www.hydrol-earth-syst-sci.net/21/1107/2017/hess-21-1107-2017.html)  
 864 [-syst-sci.net/21/1107/2017/hess-21-1107-2017.html](https://www.hydrol-earth-syst-sci.net/21/1107/2017/hess-21-1107-2017.html)
- 865 Savenije, H. H. G., & Hrachowitz, M. (2017). Catchments as meta-organism -  
 866 a new blueprint for hydrological modelling. *Hydrology and Earth System*  
 867 *Sciences*, 21(2), 1107–1116. Retrieved from [http://doi.org/10.5194/](http://doi.org/10.5194/hess-21-1107-2017)  
 868 [hess-21-1107-2017](http://doi.org/10.5194/hess-21-1107-2017)
- 869 Seibert, J., & Vis, M. (2012). Teaching hydrological modeling with a user-friendly  
 870 catchment-runoff-model software package. *Hydrology and Earth System Sci-*  
 871 *ences*, 16(9), 3315.
- 872 Silva, M., & Recalde, L. (2004). On fluidification of petri nets: from discrete to hy-  
 873 brid and continuous models. *Annual Reviews in Control*, 28(2), 253–266.
- 874 Singh, V. P., & Woolhiser, D. A. (2002). Mathematical modeling of watershed hy-  
 875 drology. *Journal of Hydrology*, 7, 270–292.
- 876 Sontag, E. (1998). *Mathematical control theory: deterministic finite dimensional sys-*  
 877 *tems*. Springer-Verlag.
- 878 Soulsby, C., Birkel, C., & Tetzlaff, D. (2016). Modelling storage-driven connectivity  
 879 between landscapes and riverscapes: towards a simple framework for long-term  
 880 ecohydrological assessment. *Hydrological Processes*, 30(14), 2482–2497.
- 881 Strogatz, S. (1994). *Non linear dynamics and chaos, with application to physics, bi-*  
 882 *ology, chemistry and engineering*. Perseus Books.

- 883 Takahashi, Y. (2005). Translation from natural language to stock flow diagrams. In  
884 *Proceedings of 23rd international conference of system dynamics society*.
- 885 Todini, E. (1988). Rainfall runoff modelling: Past, present and future. *Journal of*  
886 *Hydrology*, 100, 341352.
- 887 Wagener, T., Wheeler, H., & Gupta, H. (2004). *Rainfall-runoff modelling in gauged*  
888 *and ungauged catchments*. Imperial College Press.
- 889 Wilkinson, D. J. (2011). *Stochastic modelling for systems biology*. CRC press.
- 890 Willems, J. (2007). The behavioral approach to open and interconnected systems.  
891 *IEEE Control Systems Magazine*, December, 46-99. Retrieved from [http://](http://doi.org/10.1109/MCS.2007.906923)  
892 [doi.org/10.1109/MCS.2007.906923](http://doi.org/10.1109/MCS.2007.906923)
- 893 Yamada, T., & Foulds, L. R. (1990). A graphtheoretic approach to investigate struc-  
894 tural and qualitative properties of systems: A survey. *Networks*, 20, 427.
- 895 Zehe, E., Ehret, U., Pfister, L., Blume, T., Schrder, B., Westhoff, M., ... Kleidon,  
896 A. (2014). From response units to functional units: a thermodynamic rein-  
897 terpretation of the hru concept to link spatial organization and functioning  
898 of intermediate scale catchments. *Hydrology and Earth System Sciences*, 18,  
899 4635-4655. Retrieved from <http://doi.org/10.5194/hess-18-4635-2014>